Neurotoxicology 72 (2019) 15–28

Contents lists available at ScienceDirect

Neurotoxicology

journal homepage: www.elsevier.com/locate/neuro

Full Length Article

Modulation of caspase-3 gene expression and protective effects of garlic and spirulina against CNS neurotoxicity induced by lead exposure in male rats

Mona K. Galal[a], Ebtihal M.M. Elleithy[b], Mohamed I. Abdrabou[b], Noha A.E. Yasin[b,*], Youssef M. Shaheen[b]

[a] Department of Biochemistry, Faculty of Veterinary Medicine, Cairo University, Giza, Egypt
[b] Department of Cytology and Histology, Faculty of Veterinary Medicine, Cairo University, Giza, Egypt

ARTICLE INFO

Keywords:
Lead acetate
Garlic
Spirulina
Oxidative stress
Apoptosis
Histopathology

ABSTRACT

Lead (Pb) is a ubiquitous environmental and industrial pollutant with worldwide health problems. The present study was designed to investigate the neurotoxic effects of Pb in albino rats and to evaluate the ameliorative role of garlic as well as *Spirulina maxima* against such toxic effects. Forty adult male rats were used in this investigation (10 rats/group). Group I: served as control, Group II: rats received lead acetate (100 mg/kg), Group III: rats received both lead acetate (100 mg/kg) and garlic (600 mg/kg) and Group IV: rats received both lead acetate (100 mg/kg) and spirulina (500 mg/kg) daily by oral gavage for one month. Exposure to Pb acetate adversely affected the measured acetyl cholinesterase enzyme activity, oxidative stress and lipid peroxidation parameters as well as caspase-3 gene expression in brain tissue (cerebrum and cerebellum). Light and electron microscopical examination of the cerebrum and cerebellum showed various lesions after exposure to Pb which were confirmed by immunohistochemistry. On the other hand, administration of garlic and spirulina concomitantly with lead acetate ameliorated most of the undesirable effects. It could be concluded that, the adverse effects induced by lead acetate, were markedly ameliorated by co-treatment with *S. maxima* more than garlic.

1. Introduction

In recent years, the environmental contamination by heavy metals has increased drastically along with the rapid development of modern industry. The excessive amount of heavy metals in animals feed and feed stuffs are often due to human actions, resulting from either agricultural or industrial production or accidental or deliberate misuse (Al-Mzaien et al., 2015). Among these metals is lead (Pb), which has increased substantially during the last few years in both urban and periurban areas (Ahmed Refat and Abass, 2011). It is still added to many commercial products including paints, eye cosmetics, gasoline, enamels and water pipes (Sansar et al., 2011). Lead has extensive multifaceted action on both human and animal health with a broad range of physiological and biochemical dysfunctions (Gurer and Ercal, 2000). It is a cumulative toxicant that virtually affects multiple body systems including the neurological, hematological, gastrointestinal, cardiovascular and renal systems (Lamidi and Akefe, 2017). Compared to other organ systems, the nervous system appears to be the most sensitive and chief target for lead induced toxicity (Singh et al., 2017). With the increase in human life expectancy, the incidence of age-related neurodegenerative disorders such as Parkinson's disease, Alzheimer's disease and Huntington's disease has also increased (Borgesius et al., 2011). Despite decades of study, the exact mechanism of action of lead, a potent neurotoxic agent, has not been full elucidated and needs more declaration. One of the most suggested mechanisms of lead is the induction of apoptosis (Pulido and Parrish, 2003). As lead is a multitarget toxicant, it exerts a toxic manifestation by oxidative free radicals over production that mediates the disruption of the delicate pro- and antioxidant balance existing in mammalian cells (Lamidi and Akefe, 2017). Recently, several anti-oxidative approaches have been proposed to reduce the symptoms of lead toxicity (Mabrouk et al., 2016). In this regard, several studies have exhibited the antioxidant activities of numerous natural products against many toxic metals (Morgan et al., 2018). Plants have always been the sources of substantial medicines since time immemorial. Currently there is a huge movement and emphasis towards scientifically and clinically unlocking the value of traditional phyto-medicines in the service of humanity as well as controlling and treating diseases (Flora et al., 2012a). *Allium sativum*, or commonly known as garlic, is a versatile vegetable and medicinal plant credited to have remarkable pharmacological properties (Shalaby and Hammoda, 2015). It is a good source of dietary phytochemicals, has the ability to enhance detoxification of foreign compounds (El-Demerdash

* Corresponding author.
E-mail addresses: nohayassin428@yahoo.com, nohayassin428@cu.edu.eg (N.A.E. Yasin).

https://doi.org/10.1016/j.neuro.2019.01.006
Received 14 November 2018; Received in revised form 4 January 2019; Accepted 24 January 2019
Available online 28 January 2019
0161-813X/

et al., 2005), defending against free radical damage and protecting different organs against oxidative stress as well as inflammatory injuries in many experimental models (Salem and Salem, 2016). Extensive studies have shown garlic to be significantly effective against heavy metals poisoning (Sadeghi et al., 2013). Moreover, the beneficial effects of garlic and its constituents on neuronal physiology and brain functions have been begun to emerge in wide range (Mathew and Biju, 2008). Spirulina is referred to free-floating filamentous microalgae with spiral characteristics of its filaments (Deng and Chow, 2010). Among large number of spirulina species, *Spirulina maxima* is most intensively investigated. Spirulina species are edible with high nutritional moreover potential therapeutic values (Deng and Chow, 2010). The nutritional value of spirulina is well-known by its richness in all the 3 types of micronutrients, proteins, lipids and carbohydrate as well as phytonutrients and trace minerals (El-Tantawy, 2016; Ghaeni and Roomiani, 2016). Accordingly, it has been declared that spirulina could modify many toxicity problems induced by drugs, chemicals (Lu et al., 2010) and heavy metals (Banji et al., 2013). Extensive studies have been proven that spirulina owns several nutritional and pharmacological properties (Sharoud, 2015). Despite the above pharmacological and therapeutic properties of garlic and spirulina, there is a dearth of literature about the possible protective role of garlic or spirulina against the harms of lead acetate-induced neurotoxicity. Therefore, the present study aimed to determine whether *Allium sativum* or *Spirulina maxima* can ameliorate Pb-induced neurotoxic damage.

2. Materials and methods

2.1. Chemicals

Lead acetate trihydrate powder $(CH3\ COO)_2\ Pb{\cdot}3H_2O$ (Lupa, Indian) was purchased from El-Mekawy Company. Garlic as dried garlic powder 200 mg in each tablet (standardized to contain not less than 0.45% allicin) from ATOS pharma, was grounded and suspended in distilled water. *S. maxima* was obtained as a green odorless, water-soluble, fresh flakes from Agriculture Research Center, Cairo, Egypt. It contains protein (61.3%), carbohydrates (20%), lipid (5.8%), gamma linolenic acid (14% of total fatty acids), linoleic acid (8.7% of total fatty acids), β-carotene (1500 mg/Kg), α-tocopherols (150 mg/Kg), iron (1300 mg/Kg), zinc (26 mg/Kg), copper (11 mg/Kg) and moisture (5.2%). It was dissolved in distilled water.

2.2. Experimental protocol and animal grouping

A total of forty male albino rats, weighting about 180–200 g were obtained from the breeding unit of The Veterinary Hygiene and Management Department, Faculty of Veterinary medicine, Cairo University. These animals were housed in plastic cages at room temperature and exposed to 12 h light/dark cycle. They had access to standard rodent laboratory diet and drinking water ad libitum throughout the whole experimental period. The institutional animal care and use committee (IACUC) of Cairo University approved the protocol of the experiment (IACUC protocol no. CU-II-S-61-17). Animal experiments conformed to the guidelines of the National Institutes of Health (NIH). After two weeks of acclimatization period, they were randomly assigned into four equal groups (each containing 10 animals) according to dietary treatments applied for one month: Rats from group I (Gp I) served as untreated control and were fed with the standard diet and normal drinking water; rats from the other three groups were orally treated with lead acetate (100 mg/kg/day) according to Al-Mzaien et al. (2015) and animals in (Gp III) & (Gp IV) were additionally treated with 600 mg/kg/day *A. sativum* and 500 mg/kg/day *S. maxima* respectively for one month. All the treatments were administrated by gastric gavage. The animals were observed daily for signs of toxicity throughout the experimental period.

2.3. Sample collection and preparation

At the end of the experiment, the animals were sacrificed by cervical dislocation under light anesthesia. The brain samples were collected and stored for further analysis.

2.4. Biochemical investigation

Both cerebrum and cerebellum samples were homogenized in 10% (W/V) cold phosphate buffer pH 7.4 and centrifuged at 4000 rpm for 20 min. The resulting supernatant was used for biochemical assessments. Malondialdehyde (MDA) was estimated according to Ohkawa et al. (1979). The MDA level was determined by thiobarbituric acid reactive substances (TBARS) formation and measured spectrophotometrically at 532 nm. Superoxide dismutase (SOD) enzyme activity was determined according to Nishikimi et al. (1972). Catalase (CAT) enzyme activity was determined by a colorimetric method according to Aebi (1984). Acetyl cholinesterase (AChE) enzyme activity was measured according to Knedel and Böttger (1967). Protein level was determined spectrophotometrically at 595 nm using bovine serum albumen protein standard according to Bradford dye-binding assay (Bradford, 1976). All those parameters were assayed in both cerebrum and cerebellum using commercial assay kits from bio-diagnostic company, Egypt.

2.5. Quantitative real-time PCR for caspase-3 gene

Approximately 100 mg of either cerebrum or cerebellum tissues were used for total RNA extraction using total RNA Extraction Kit (Vivantis, Cat. No. GF-TR- 050). Concentration and purity of total RNA samples were measured by Nanodrop. Approximately 2 µg of total RNA was reverse transcribed using reverse transcriptase enzyme (RT) in a 20 ml reaction mixture containing oligo-(dT)-primer, Rnase inhibitor, dNTP mix and 5X reaction buffer (Omniscript RT kit, Invitrogen). The mRNA expression level of the apoptotic gene caspase-3 gene was determined using real-time quantitative polymerase chain reaction (qRT-PCR). Sybr green master mix (Thermo Scientific) was used according to standard protocol, and the primers were designed using Primer 3 software; Caspase-3 forward primer: 5'- CAT GCA CAT CCTCAC TCG TG -3', reverse: 5'- CCC ACT CCC AGT CAT TCC TT -3'. The cDNA was amplified by 40 cycles of denaturation at 95 °C for 30 s, annealing at 60 °C for 30 s and extending at 72 °C for 30 s. The Beta-actin gene was amplified during the same reactions to serve as a reference gene according to Rashad et al. (2018). Duplicate plates were tested, and cycle threshold (Ct) values were used to calculate the gene/ Beta-actin ratio, with a value of 1.0 used as the control (calibrator). The normalized expression ratio was calculated using the $2^{-\Delta\Delta Ct}$ method as described by Livak and Schmittgen (2001).

2.6. Histopathological examination

2.6.1. Light microscopy

At the end of experiment, the whole brain tissues were rapidly obtained from the rats in different groups and immediately fixed in 10% neutral buffered formalin (NBF) for (24–48 h). After proper fixation, the samples were dehydrated in ascending dilutions of alcohol. Specimens were cleared in xylene, embedded in paraffin and cut at 4 µm to obtain paraffin sections. De-waxed serial sections were subjected to be studied by hematoxylin and eosin stain for histopathological examination (Bancroft and Gamble, 2008).

Four point scoring system (ordinal method) was used to express the degree of severity of the observed histopathological alterations in both cerebral and cerebellar tissues as follows: normal histological structure (-), mild (+), moderate (++) and severe (+++) damage. 5 slides from 5 different rats from each group were examined for grading of the following pathological injuries: neuronal degeneration and necrosis,

perineuronal vacuolation and edema, perivascular (Virchow-Robin) space, cerebral and cerebellar hemorrhage and congestion of blood vessels. The severity of various pathological lesions in different groups of rats was assigned according to the number of affected slides as well as the number of affected regions within the same slide. The individual score for each animal was determined and then the mean score for each group was calculated for various pathological injuries (Haridy et al., 2014; Chaâbane et al., 2017).

2.6.2. Immunohistochemical examination for caspase-3

Immunohistochemistry was performed on paraffin sections and mounted on positively charged slides for detection caspase-3 as a marker for apoptosis using avidin-biotin-peroxidase complex (ABC) method (Hsu et al., 1981). Antibodies used in immunohistochemistry (IHC) include: anti-caspase-3 antibody and active (cleaved) form produced in rabbit (AB3623, EMD Millipore). Briefly, brain sections were incubated with antibodies mentioned above and the reagents required for ABC method (Vectastain ABC-HRP Kit, Vector Laboratories) were added. Each marker expression was labeled with peroxidase and colored with diaminobenzidine substrate (DAB, Sigma) for detection of antigen-antibody complex.

Immunohistochemically stained sections were examined using Leica Qwin 500 analyzer computer system (Leica Microsystems, Switzerland) in Faculty of Dentistry, Cairo University. The image analyzer was calibrated automatically to convert the measurement units (pixels) produced by the image analyzer program into actual micrometer units. Caspase-3 immunostaining were measured as area % in a standard measuring frame in five fields in each group using magnification (x400) by light microscopy transferred to the screen. The areas showing caspase-3 positive brown immunostaining were chosen for evaluation regardless the intensity of staining. Mean value and standard deviation were obtained for each specimen.

2.6.3. Electron microscopy

Brain tissues (cerebellum and cerebral cortex) from each group were immediately placed in 3% glutaraldehyde in 0.1 M phosphate buffer for a few hours and post fixed in 1% osmium tetroxide for one hour. Semithin Sections (1 μm) were prepared and stained with toluidine blue. Ultrathin sections of 50 nm were cut by an ultra-microtome from selected areas, were contrasted with uranyl acetate and lead citrate and were photographed with transmission electron microscope (JEOL 1010) at the Regional Center for Mycology and Biotechnology (RCMP), Al-Azhar University.

2.7. Statistical analysis

The results were expressed as mean ± SD. Data were analyzed using one-way analysis of variance (ANOVA) to determine the significance of the mean between the groups followed by LSD post hoc test (SPSS 16.0). P-value < 0.05 was considered statistically significant.

3. Results

3.1. Oxidative stress parameters

A significant elevation in MDA level was observed in both cerebrum and cerebellum from lead-exposed rats (Gp II) as compared with control (Gp I) group. On the other hand, administration of garlic (Gp III) or spirulina (Gp IV) revealed a significant decrease in MDA levels by 38.1% and 48.28% for cerebrum and by 38.94% and 47.95% for cerebellum, respectively (Fig. 1A). Concerning the oxidative stress markers levels, significant reductions in brain SOD and CAT activity were detected in lead-exposed rats compared with those of control group (Fig. 1B & C). In contrast the garlic co-treatment significantly retrieved those altered levels of the antioxidants by 30.6% in cerebrum and 30.98% in cerebellum for SOD and by 19.73% in cerebrum and 20.14% in cerebellum for CAT, respectively. While spirulina co-treatment significantly retrieved those altered levels of the antioxidants by 44.09% in cerebrum and 44.11% in cerebellum, respectively, for SOD and by 26.46% in cerebrum and 27.06% in cerebellum, respectively, for CAT.

3.2. Acetylcholinesterase enzyme activity

Gp II treated with lead showed a significant decrease in the AChE activity in the brain tissues as compared to the Gp I (Fig. 2). On the other hand, the co-administration with garlic (Gp III) /or spirulina (Gp IV) induced significant elevation in cerebrum and cerebellum AChE activity by 39.68% and 43.95% and by 54.73% and 60.49%, respectively as compared to Gp II. These results indicated that both garlic and spirulina had partial recovery effect on brain AChE activity.

3.3. Quantitative real-time PCR for caspase-3 gene

To determine the effects of lead on cell apoptosis in both cerebrum and cerebellum, we investigated the expression of apoptosis factor caspase-3 mRNA gene expression (Fig. 3). As showed in the obtained results, lead intoxication (Gp II) significantly promoted up-regulation of apoptosis related gene Caspase-3 compared to (Gp I) in both cerebrum and cerebellum. Co-administration of spirulina down regulates the Caspase-3 expression by 69.8% in cerebrum and 62.12% in cerebellum. While, garlic reduced the expression level by 38.8% in cerebrum and 37.87% in cerebellum (Fig. 3).

3.4. Histopathology and immunohistochemistry

3.4.1. Light microscopical examination

3.4.1.1. A. Cerebrum. Cerebral cortex from (Gp I) showed normal structure and distribution of neurons (Fig. 4A & B), deep to this layer cerebral white matter composed of unmyelinated nerve fibers going to and coming from the cortex.

The microscopic examination of cerebral stained sections from (Gp II) revealed deleterious histopathological changes in all layers as compared with (Gp I). It showed congested and edematous meninges. Brain edema was evidenced by dilated Virchow-Robin spaces (Fig. 4 C).The neuropil among the neurons and neuroglia cells showed sever vacuolation of variable sizes either single or multiple with perineural and perivascular edema (Fig. 4D & 4E). The blood capillaries revealed disruption of their wall. Both pyramidal and granular cells were affected. Some pyramidal cells were shrunken with some dystrophic changes in the form of pyknotic hyperchromatic nuclei and wide perineural spaces (Fig. 4D). While other neurons were shrunken and loss of their process with hyperbasophilia and dark stained nuclei. Neuronal degeneration, chromatolysis and basophilic coagulative necrosis were observed in most sections with or without neurophagia (Fig. 4E) (see Table 1).

On the other hand, examination of (Gp III) showed noticeable improvement in the histological architecture. The neuropil was still vacuolated with some perineural and perivascular space. Some pyramidal cells were shrunken, distorted with pyknotic nuclei and pericellular halos while others appeared normal. Other neurons were faintly stained, vacuolated, loss of their Nissl granules with karyolysis (Fig. 5A).

Examination of cerebral sections obtained from (Gp IV) revealed considerable improvement in neurocytes, neuroglia as well as neuropil with absence of meningitis. Most neurocytes appeared nearly normal as in control group with central large vesicular nuclei that contained one or two nucleoli and peripheral distribution of Nissl granules (Fig. 5B). Hardly found affection in the neuroglia.

3.4.1.2. B. Cerebellum. Examination of cerebellar sections obtained from control group revealed normal histological architecture. It composed of folia which contained a central core of white matter

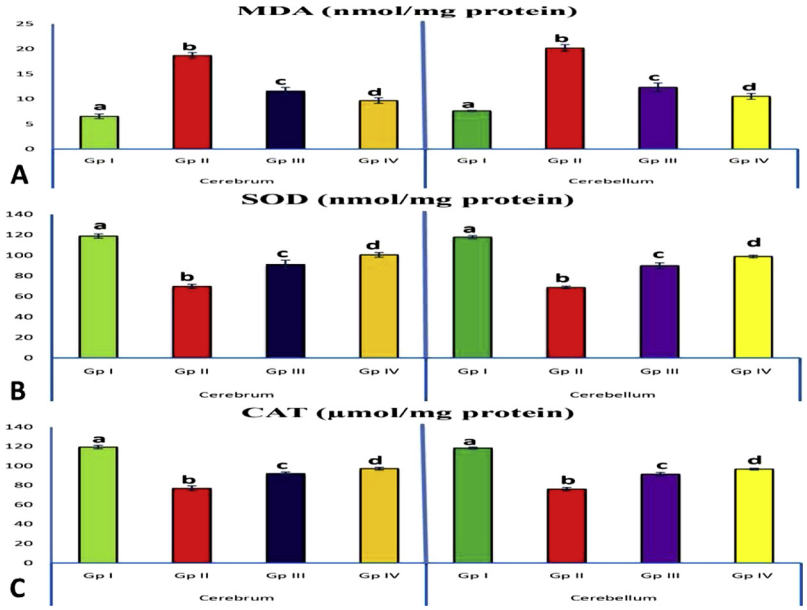

Fig. 1. Protective influence of garlic or spirulina on the oxidative stress parameters against lead acetate induced neurotoxicity. Values are presented as mean ± SD (n = 5 rats / group). Data were expressed as means ± S.D. Groups having different letters are significantly different.

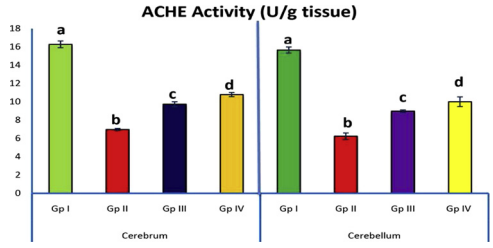

Fig. 2. Protective influence of garlic or spirulina on Acetylcholinesterase enzyme activity against lead acetate induced neurotoxicity. Values are presented as mean ± SD (n = 5 rats / group). Data were expressed as means ± S.D. Groups having different letters are significantly different.

covered by a cortex of gray matter. The cerebellar cortex showed trilaminar arrangement of neurons; outer molecular layer, inner granular layer and a row of Purkinje cell layer in-between (Fig. 6A). Light microscopic examination of (Gp II) showed spongiosis of molecular layer. Purkinje layer was the most affected layer showing degenerated Purkinje cells with dystrophic changes in the form of shrunken cells with irregular outlines and pyknotic hyperchromatic nuclei. Some cells appeared dark with hyperbasophilia while others loss their Nissl substances with widening perineural spaces (Fig. 6B). There was substantial reduction in overall population of Purkinje cells when compared with control group. Both granular and neuroglia cells were darkly stained when compared with control group. White matter showed sever demyelination with axonal swelling indicated with sever vacuolation. On contrary, examination of sections from (Gp III) revealed improvement of the histopathological alterations in cerebellar tissues except pyknosis of few Purkinje cells with some perineural spaces and vacuolation in both Purkinje layer and white matter (Fig. 6C). On the other hand, (Gp IV) showed nearly normal structure similar to control group with well-defined Purkinje cells and ill-defined perineural spaces and vacuolation (Fig. 6D).

3.4.2. Immunohistochemistry

Immunohistological sections from control group stained for caspase-3 revealed negative immunostaining reaction in all areas of the cerebral and cerebellar cortex. On the other hand, remarkable number of apoptotic neurons and neuroglia cells showed strong positive immunoreactivity (brown immunoreaction staining of both nucleus and cytoplasm) in lead exposed animals when compared with control group; where sections from animals co-treated with garlic demonstrated a clear reduction in the caspase-3 positive apoptotic cells. Meanwhile, the concurrent administration of Spirulina with lead acetate revealed nearly all neurocytes and neuroglia cells with negative immunoreactivity except very few cells (Figs. 7 and 8). Likewise, data analysis showed that lead-exposed group displayed a significant increase in the number of caspase-3 positive cells in the cerebral and cerebellar cortex compared with control group. These percentage

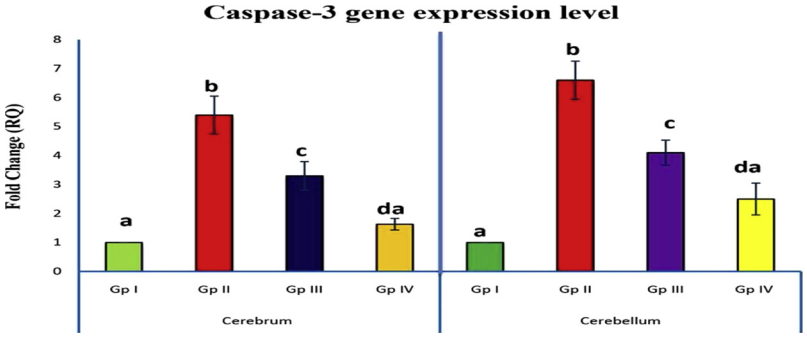

Fig. 3. Graphical representation of mRNA expression of caspase-3 gene in different experimental groups in both cerebrum and cerebellum regions estimated by qPCR. Data are represented as mean ± SD (n= 5 rats / group). Different superscripts are significantly different from each other.

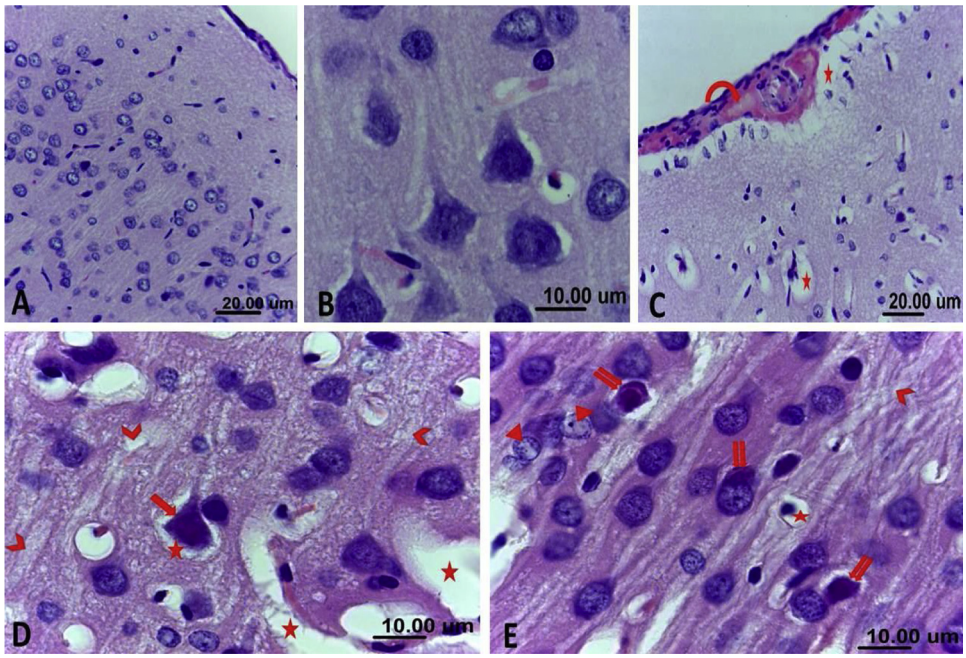

Fig. 4. A photomicrograph showing the cerebral cortex in different groups of rat. **A & B:** Control group showing neurons with large, rounded or ovoid, open face nuclei and normal distribution of cytoplasm. **C:** Lead-exposed group showing edema, congestion, and hemorrhage of the meninges (circle arrow), perivascular and pericellular spaces (star). **D:** Lead-exposed group revealed shrunken pyramidal cell with pyknotic hyperchromatic nucleus and densely stained cytoplasm (arrow). The neuropil showed persistent vacuoles of variable size (edema) (chevron). Perivascular and pericellular spaces were noticed (star). **E:** Lead-exposed group illustrating neuronal degeneration as different neurons were darkly stained, irregular, distorted and shrunken, loss of their process with dark stained nuclei and hyperbasophilia (double arrow). Some cells showed chromatolysis with coagulative necrosis (triangle). Also, vacuoles (chevron), perivascular and perineural spaces were observed (star) (H & E).

Table 1
Microscopic scoring of neuropathological lesions in different groups of rats. Scoring was classified according to severity of lesions into: (-) none, (+) mild, (++) moderate and (+++) severe damage (n = 5 rats/ group).

	Gp I	Gp II	Gp III	Gp IV
Neuronal degeneration and necrosis	–	+++	++	+
Perineuronal vacuolation and edema	–	+++	++	+
Perivascular (Virchow-Robin) space	–	+++	++	+
Cerebral and cerebellar hemorrhage	–	++	–	–
Congestion of blood vessels	–	++	+	–

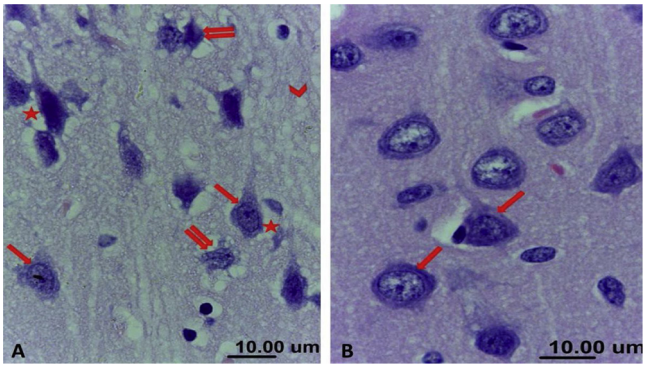

Fig. 5. A photomicrograph showing the cerebral cortex in different groups of rat. **A:** Garlic co-treated group revealed some neurons were apparently normal (arrow) while others were degenerated with chromatolysis and necrosis (double arrow). Residual vacuolations (chevron) and perineural spaces (star) were also noticed. **B:** Spirulina co-treated group showed nearly normal morphological appearance of neurons (arrow) as in control group (H & E).

significantly decreased in the number in the cerebral and cerebellar cortex of -garlic-treated groups by 64.92% and 60.62%, -spirulina-treated group by 80.81% and 78.55%, respectively (Fig. 9).

3.4.3. Electron microscopy

3.4.3.1. A. Cerebrum. Ultra structure examination of cerebral section from control group revealed normal cytoarchitecture. Neurons exhibited large electron lucent nuclei with well-defined nucleuolus. The cytoplasm displayed numerous rER, polysomes and tubular or spherical mitochondria with well-defined cristae (10 A, B and C). Also, neuroglia cells appeared with large nuclei and scanty cytoplasm supporting other neurons. Nuclei contained dispersed chromatin and peripheral arranged heterochromatin (10 A). Blood vessels were engorged with blood (10C). The surrounding neuropil showed multiple myelinated and unmyelinated nerve fibers, neuroglia cells and blood capillaries. The myelinated nerve fibers had regular compact myelin sheath.

Ultrastructure examination of cerebral section from Gp II illustrated neurons with sever degeneration. Some neurons showed shrinkage in the nuclei with different degree of pyknosis and invaginations of their outlines with wide perinuclear spaces. Their cytoplasm contained dilated rER and swollen vacuolated mitochondria with complete loss of cristae (Fig. 10D). Other degenerated neurons revealed nuclear condensation and their vacuolated cytoplasm displayed swollen mitochondria with disrupted cristae. Myelinated nerve fibers were also noticed with splitting and irregular arrangement of myelin sheath (Fig. 10E). Blood vessels were congested and surrounded with markedly enlarged processes of astrocytes. Some myelinated nerve fibers appeared with regular myelin sheath while other were observed with irregular discontinuous myelin (Fig. 10F).

Ultrastructure examination of cerebral section from Gp III exhibited some neurons with nearly normal structure while others were still degenerated. Some cells appeared with large spherical euchromatic nuclei and their cytoplasm contained rER and mitochondria with well-defined cristae. Other cells appeared with pyknotic nuclei and vacuolated cytoplasm. Myelinated nerve fibers with regular myelin sheath were also noticed (Fig. 11A). Another nerve cells exhibited spherical nuclei with clumps of peripheral heterochromatin and dilated rER. The neuropil contained many nerve fibers with irregular interrupted myelin sheath (Fig. 11B). Blood vessels were congested with blood and surrounded with markedly enlarged feet of astrocytes (Fig. 11C).

Ultrastructure examination of cerebral section from Gp IV demonstrated nearly normal neurons similar to Gp I. Some neuron observed with large spherical electron lucent nucleus and well-defined cytoplasmic organelles. The axon hillock and initial part of axon were noticed with regular distribution of neurofilament (Fig. 11D). Other neuron appeared with dense cytoplasm contained large euchromatic nucleus with well-defined nucleolus, abundant rER, many free

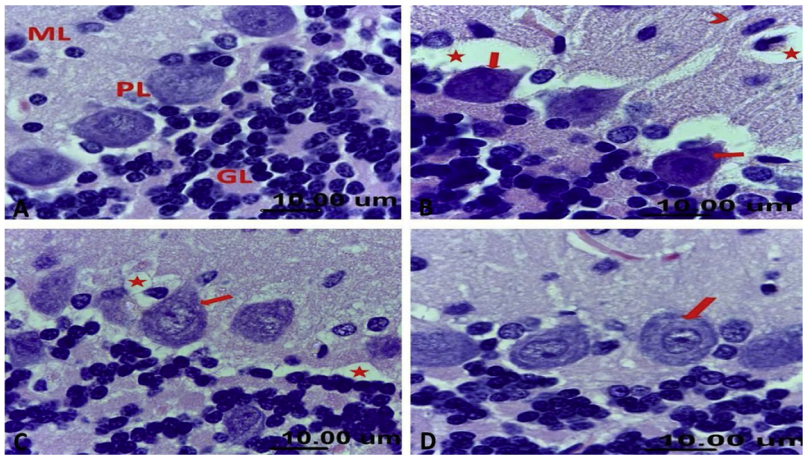

Fig. 6. A photomicrograph showing the cerebellar cortex in different groups of rat. **A:** Control group showing trilaminar arrangement of neurons in the form of outer molecular layer (ML), middle Purkinje layer (PL) and inner granular layer (GL). **B:** Lead-exposed group showing shrunken pyknotic darkly stained Purkinje cells (arrow) with perineural halos (star). The molecular layer showed spongiosis (chevron) while cells of granular layer were darkly stained. **C:** Garlic co-treated group revealed nearly normal Purkinje cells but with residual perineural spaces (star) and vacuolation in molecular layer. **D:** Spirulina co-treated group showed Purkinje cells resemble to control with large vesicular central nucleus, prominent deeply stained nucleolus and basophilic granular cytoplasm (arrow) (H & E).

ribosomes and mitochondria (Fig. 11E). The surrounding neuropil exhibited multiple nerve fibers either myelinated with regular compact myelin sheath or unmyelinated (Fig. 11F).

3.4.3.2. B. Cerebellum. The ultrastructure examination of cerebellar sections of Gp I was similar to the normal electron microscopic pictures. Purkinje cells were characteristically very large neurons observed in-between molecular and granular layers (Fig. 12A). Their nuclei appeared large contained electron lucent, homogeneously dispersed euchromatin and small granules of heterochromatin with well-defined nucleolus. Their cytoplasm was abundant and contained well-developed Golgi apparatus, rER, polyribosomes and numerous mitochondria (Fig. 12B). Cells of granular layer were aggregated in groups with their membranes contiguous to each other. Some cells revealed cytoplasm with few mitochondria, few rER, ribosomes and rounded or ovoid euchromatic nuclei with small peripheral heterochromatin. While other cells were characterized by electron dense nuclei with clumped heterochromatin. Their processes were extending along the cell membrane of other cells of granular layer. Furthermore, myelinated nerve fibers were also observed with regular myelin sheath (Fig. 12C).

The ultrastructure examination of cerebellar sections of Gp II revealed several degenerative changes. Purkinje cells appeared as dark neuron with marked degenerative cytoplasm including disintegrated and dilated endoplasmic structures, vacuolated mitochondria and pyknotic nuclei. Moreover, pericellular and perivascular spaces were observed (Fig. 12D). The granular layer demonstrated some cells with shrunken electron dense nuclei, some irregularities in nuclear membrane and perinuclear spaces (Fig. 12E) while other cells appeared with vacuolated disintegrated cytoplasm and peripheral condensation of heterochromatin in their nuclei (Fig. 12E and F). Mitochondria were observed with pronounced degenerative changes. Some mitochondria resembled double-contoured, balloon-like electron-lucent vacuoles while others were appeared with partial or complete loss of cristae. Myelinated nerve fibers were also noticed with splitting discontinuous myelin sheath and irregular distribution of neurofilament (Fig. 12F). The white matter revealed cells with vacuolated cytoplasm and different degree of pyknosis. Many myelinated nerve fibers observed with vacuolation and loss of myelin sheath (Fig. 12G).

Ultrastructure examination of cerebellar sections from Gp III illustrated some changes of partial recovery. Purkinje cells appeared nearly normal with abundant cytoplasm contained well-developed organelles and euchromatic nuclei with invaginated envelope for a variable distance forming either shallow indentation or deep invagination (Fig. 12H). The white matter exhibited cells with vacuolated cytoplasm, many ribosomes, mitochondria with well-defined cristae and nucleus with dispersed chromatin and peripheral heterochromatin. Moreover, many myelinated nerve fibers were noticed with regular myelin sheath and some with discontinued one (Fig. 12I).

The ultrastructure examination of cerebellar sections of Gp IV did not demonstrate any substantial differences with control group especially granular cell layer (Fig. 12J). Cells of granular layer showed abundant cytoplasm contained numerous rER, polyribosomes, mitochondria with well –defined cristae and large ovoid euchromatic nuclei (Fig. 12K) while other showed nuclei with fine dispersed chromatin and clumps of peripheral heterochromatin (Fig. 12L).

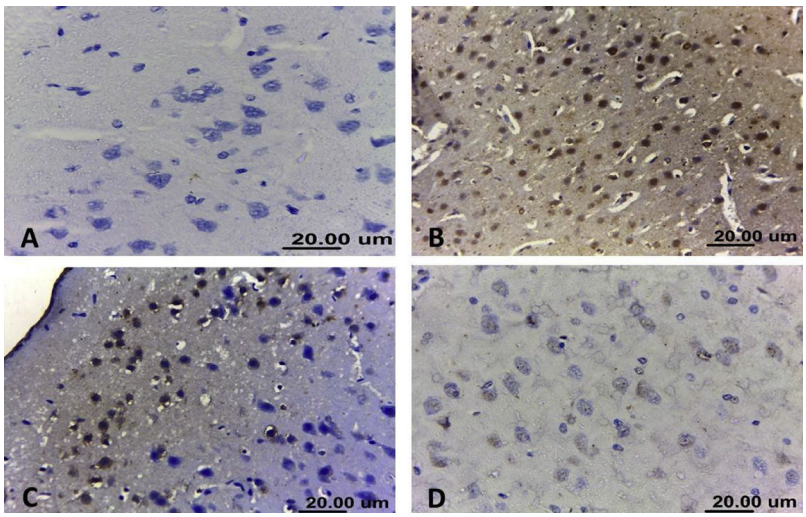

Fig. 7. A photomicrograph showing the immunohistochemical staining of caspase-3 expression of the cerebral cortex in different groups of rat. **A:** Control group showing negative immunoreactivity in both neurons and neuroglia cells. **B:** Lead-exposed group demonstrating strong positive immunoreactivity. **C:** Garlic co-treated group revealing some cells were caspase-3 positive while others were negative. **D:** Spirulina co-treated group showing most of the cells were caspase-3 negative and very few cells were positive with weak reaction (Caspase-3).

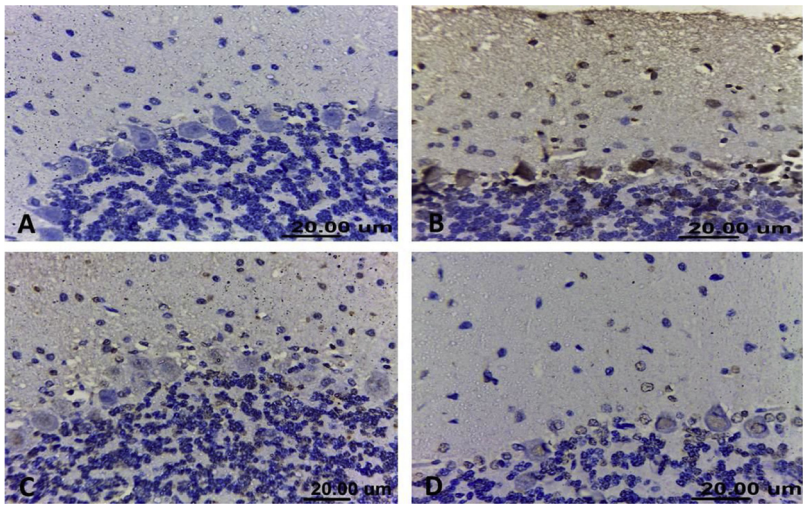

Fig. 8. A photomicrograph showing the immunohistochemical staining of caspase-3 expression of the cerebellar cortex in different groups of rat. **A:** Control group showing negative caspase-3 expression. **B:** Lead-exposed group demonstrating strong positive immunoreactivity especially in Purkinje cells. **C:** Garlic co-treated group revealing some cells were caspase-3 positive while others were negative. **D:** Spirulina co-treated group showing most of the cells were caspase-3 negative and very few cells were positive with weak reaction (Caspase-3).

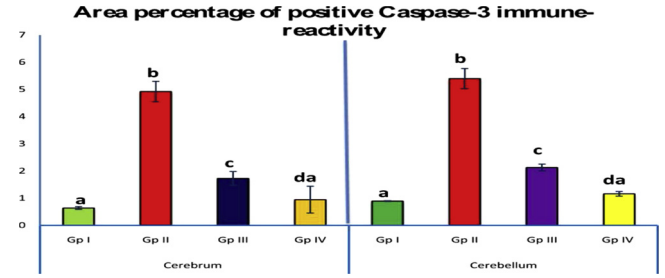

Fig. 9. A photomicrograph showing the area percentage of caspase-3 immune-reactivity of the cerebral and cerebellar cortex in different groups of rat. Values are presented as mean ± SD (n = 5 fields / group). Data were expressed as means ± S.D. Groups having different letters are significantly different.

4. Discussion

A number of research studies have revealed that exposure to lead is extremely dangerous and results in a variety of neurological disturbances (Singh et al., 2017). Regarding our results of the oxidative stress markers, it was observed that lead acetate administration had an adverse effect on oxidative stress markers in addition to concomitant reduction in CAT and SOD enzymes activity in brain tissue compared to control which suggesting that the oxidant /antioxidant balance in brain tissue of rats was disrupted by lead administration (Singh et al., 2017). MDA is a substantial oxidation product of peroxidation of poly-unsaturated fatty acids. Consequently, escalated MDA level is an essential LPO indicator (Durak et al., 2010) which is an index for oxidative stress damaging the cell membrane and altering membrane fluidity. The recorded significant increase in MDA level following lead exposure are in accordance with those obtained by Wang et al. (2013)

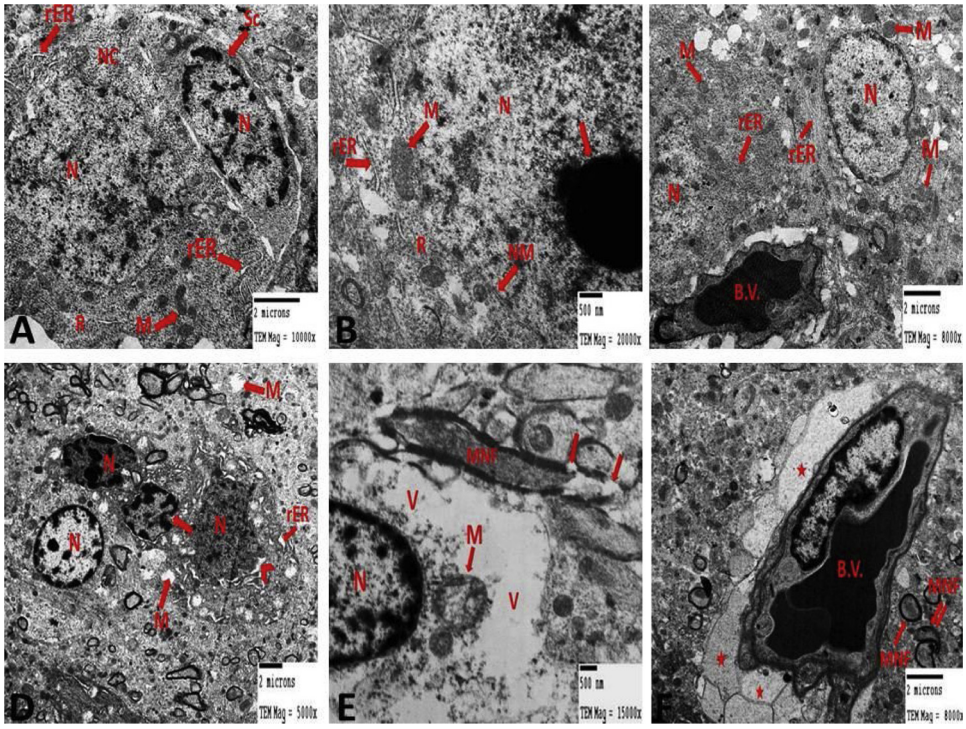

Fig. 10. Electron micrographs of cerebral sections from different groups of rats. **A:** Gp I showed nerve cell (NC) with large euchromatic nucleus (N), normal nuclear envelope, numerous rER, polyribosomes (R) and spherical mitochondria (M) with well-defined cristae. Supporting neuroglia cells (SC) with large nucleus (N), scanty cytoplasm. **B:** Gp I demonstrated neuron with large electron lucent nucleus (N), well-defined nucleolus (arrow), normal nuclear membrane (NM), rER and elongated mitochondria with well-defined cristae (M). **C:** Gp I illustrated some neuron with euchromatic nucleus (N) and other with dispersed chromatin and peripheral heterochromatin (N), numerous rER and spherical mitochondria (M). Blood vessel (B.V.) was engorged with blood. **D:** Gp II revealed shrunken nuclei (N) with different degree of pyknosis, invaginations in their outlines (arrow), wide perinuclear spaces (chevron), dilated rER and swollen vacuolated mitochondria with complete loss of cristae (M). **E:** Gp II revealed degenerated neuron with nuclear condensation (N), vacuolated cytoplasm (V), swollen mitochondria (M) with disrupted cristae. Notice the myelinated nerve fiber (MNF) with splitting with irregular arrangement of myelin sheath (arrow). **F:** Gp II showed blood vessel (B.V.) surrounded with markedly enlarged processes of astrocytes (star). Some myelinated nerve fibers (MNF) appeared with regular myelin sheath (arrow) while other were with irregular discontinued myelin (double arrow).

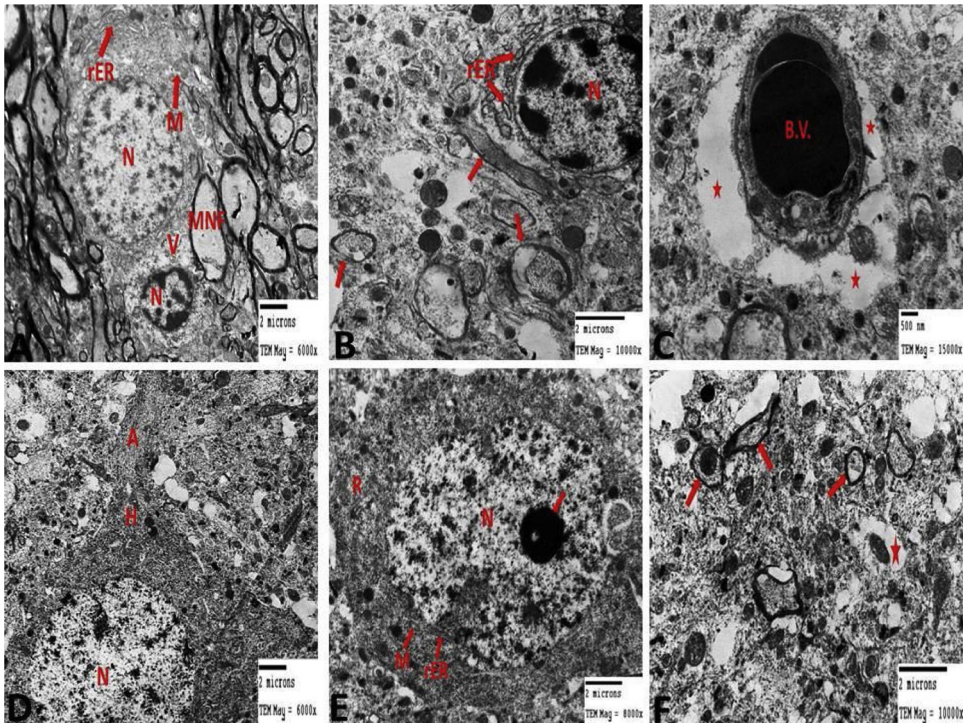

Fig. 11. Electron micrographs of cerebral sections from different groups of rats. **A:** Gp III exhibited nearly normal neuron with large spherical euchromatic nucleus (N), well-developed rER and mitochondria (M) with well-defined cristae. Other shrunken cell was observed with pyknotic nucleus (N) and vacuolated dissoluted cytoplasm (V). Notice myelinated nerve fiber (MNF) with regular myelin sheath. Fig. 11B demonstrated nerve cell with dilated rER and spherical nucleus (N) with clumps of peripheral heterochromatin. The neuropil contained many nerve fibers with irregular interrupted myelin sheath (arrow). Fig. 11C showed congested blood vessel (B.V.) and surrounded with enlarged feet of astrocytes (star). **D:** Gp IV demonstrated nearly normal neuron with large spherical electron lucent nucleus, well-defined cytoplasmic organelles, axon hillock and initial part of axon (A) with regular distribution of neurofilament. Fig. 11E showed cell with dense cytoplasm contained large euchromatic nucleus (N), well-defined nucleolus (arrow), abundant rER, many free ribosomes (R) and mitochondria (M). **F:** Gp IV illustrated neuropil with multiple nerve fibers either myelinated with regular myelin sheath (arrow) or unmyelinated.

and Abdulmajeed et al. (2016). This elevation may be attributed to the formation of highly reactive hydroxyl (OH) radical which abstracts a hydrogen (H) ion from a fatty acid resulting in the formation of a fatty acid radical. The cumulative effect of these radicals results in the weakening of membrane integrity of cells leading to cellular damage (Thuppil and Tannir, 2013). The generation of free radicals is associated with the enhanced oxidative stress following exposure to lead (Singh et al., 2017). The significant reduction in SOD and CAT activity after lead exposure comes in accordance with Al-Mzaien et al. (2015) and Abdulmajeed et al. (2016). This inhibition may be attributed to lead which exists as a bivalent cation and has electron sharing abilities resulting in covalent attachments with –SH groups of various antioxidant enzymes such as SOD, CAT and GPx (Ercal et al., 2001; Patra et al., 2011). The brain tissue is particularly vulnerable to oxidative stress because of its high oxygen consumption rate, low mitotic rate, richness in unsaturated lipids content, relatively high abundance of redox-capable transition metal ions, and relatively low availability of antioxidant enzymes compared with other organs and extended axonal morphology (Khalaf et al., 2012). These factors perhaps explain why lead exposure affects brain more than any other organ. Cognition functions and motor activities of the brain are controlled by acetylcholine, AChE and choline acetyl transferase. The effects of lead exposure on brain functions was assessed by evaluation of AChE activity, a pivotal enzyme involved in cholinergic neurotransmission. In addition, it is also known that the vital role of this enzyme in diseases with an increasing incidence in the elderly population, like Alzheimer disease (Richetti et al., 2011). In the present study, upon lead acetate a progressive decrease in ACHE activity in brain tissue was observed and our findings are in line with those mentioned by Ani et al. (2007). Inhibition of ACHE enzyme activity can be due to a deficiency of the enzyme synthesis by the inhibitory action of toxicants (El-Demerdash and Elagamy, 1999). It has been shown that lead has chemical similarity to calcium which allows lead access to critical cellular pathways, particularly within the mitochondria and in second messenger systems, where it competitively antagonizes calcium action (Onunkwor et al., 2004). Lead also has been shown to reduce enzyme activity including AChE and Na^+/K^+ ATPase activity. Therefore, lead probably changes the binding kinetics of Na^+/K^+ ATPase activity that plays an original role in linking the extracellular signals to intracellular at the neurons and also affects cholinergic transmission (Yallapragada et al., 2003). Lead may act in a mimetic role and activate the calcium mediated synaptic vesicle release mechanisms. In addition, lead competes with calcium for common binding sites and is incorporated into calcium transport systems in the nervous system, where it is important for neurotransmitter release and regulation (Devi et al., 2005). Additionally, Pb interfering with Ca^{2+} calmodulin mediated neurotransmitter release and this responsible for behavioral impairment (Gill et al., 2003; Abeer, 2012).

Suszkiw (2004) showed that Pb affected both the release and reuptake of several neurotransmitters controlled by voltage-gated Ca^{2+} channels. Pb, also, causes hyper-phosphorylation and α-synuclein accumulation, leading to the enhancement of type I (apoptosis) and type II programmed cell death (autophagy) (Zhang et al., 2012). To determine the mechanism of Pb-induced apoptosis, we examined the expression of apoptotic protein caspase-3. Lead intoxication, in the present study, caused marked increase in neural caspase-3 gene expression and protein which was consistent with previous report (El-Tantawy, 2016). Apoptosis induced by lead may be attributed to ROS–mediated mitochondrial damage and disruption of mitochondrial permeability resulting in release of cytochrome C and caspase activation (Orrenius et al., 2007). Continuous lead exposure over a long time will make ROS and antioxidants within the body become imbalanced, thus leading to oxidative stress. Oxidative stress will destroy DNA, and then stimulate apoptosis through intrinsic pathways. Flora et al. (2007) stated that lead can resemble calcium increase intracellular metabolism which is able to stimulate mitochondrial depolarization which induced release of cytochrome C that soon binds with Apaf-1, activate caspase-9, and activate caspase-3 as an executor caspase, and finally, apoptosis occurs (Flora et al., 2007). This is supported by Xu et al. (2006) and Ahmed et al. (2013) who found that lead elicits DNA damage and apoptosis, accompanied by an increase in the Bax/Bcl-2 ratio and caspase-3 activity. Kiran Kumar et al. (2009) showed that lead induces region-specific response of expression in apoptotic proteins; Bcl-2 and caspase-3. Indeed, extensive experimental studies have reported of lead induced selective apoptosis in rat brain (Dribben et al., 2011).

Examination of brain sections by light and electron microscopy, in

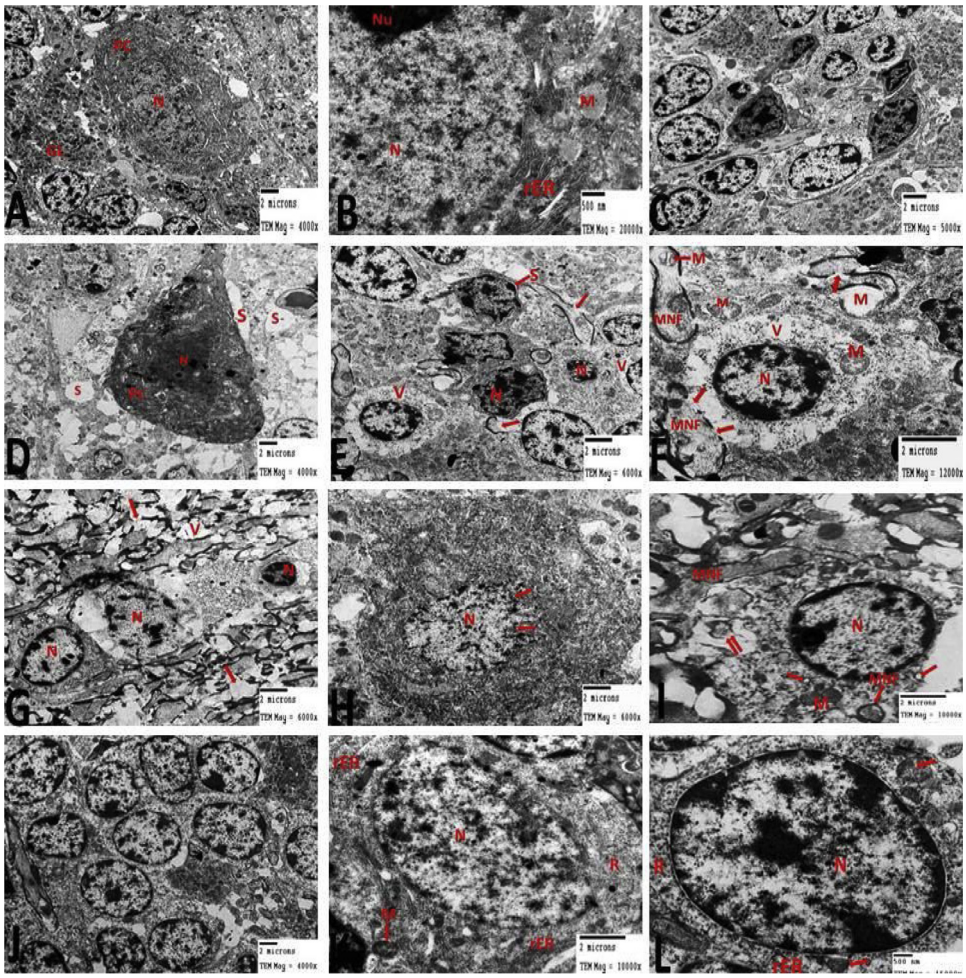

Fig. 12. Electron micrographs of cerebellar sections from different groups of rats. **A:** Gp I showed Purkinje cell (Pc) was in the vicinity cells of granular layer (GL). **B:** Gp I revealed Purkinje cell with large electron lucent nucleus (N), well-defined nucleolus (Nu), abundant cytoplasm, rER, polyribosomes and numerous mitochondria (M). **C:** Gp I illustrating different cells of granular layer and myelinated nerve fibers with regular myelin sheath. **D:** Gp II exhibited degenerated Purkinje cell (Pc), disintegrated cytoplasm, shrunken pyknotic nucleus (N), pericellular and perivascular spaces (S). **E:** Gp II exhibited cells with granular layer with shrunken electron dense nuclei (N), some irregularities in nuclear membrane and perinuclear spaces (S) while others appeared with vacuolated cytoplasm (V). Myelinated nerve fibers also noticed with splitted myelin sheath (arrow). **F:** High magnification on one degenerated cell from Gp II revealed vacuolated disintegrated cytoplasm (V), swollen mitochondria with partial loss of cristae (M), nucleus (N) with peripheral condensation of heterochromatin. Also, some mitochondria (M) resembled double-contoured with balloon-like electron-lucent vacuoles were observed. Myelinated nerve fibers were also noticed with discontinuous myelin sheath (arrow) and irregular distribution of neurofilament. **G:** Section of white matter from Gp II revealed nuclei (N) of cells with different degree of pyknosis and dissoluted cytoplasm. Many myelinated nerve fibers observed with vacuolation (V) and loss of myelin sheath (arrow). **H:** Gp III illustrated nearly normal Purkinje cell with abundant cytoplasm contained well-developed organelles and euchromatic nucleus (N) with invaginated envelope (arrow). Fig. 12I demonstrated cell in white matter with vacuolated cytoplasm (arrow), many ribosomes, mitochondria with well-defined cristae (M) and nucleus with dispersed chromatin and peripheral heterochromatin (N). Moreover, many myelinated nerve fibers were noticed with regular myelin sheath and some with discontinued one (double arrow). **J:** Gp IV showed aggregated cells of granular layer were in groups with their membranes contiguous to each other and myelinated nerve fibers with regular myelin sheath. **K and L:** Gp IV illustrated cells from granular layer with abundant cytoplasm contained many rER, polyribosomes (R), mitochondria (M) with well-defined cristae and large ovoid euchromatic nucleus (N) (12 K) or with heterochromatic nucleus (N) (12 L).

our study, did not demonstrate substantial differences among rats in control and spirulina co-treated groups and it was similar to the normal cytoarchitecture while those of garlic co-treated group showed some affections. On the other hand, lead administration displayed histological alterations in the meninges, neurons, neuroglia as well as neuropil of the brain tissues in association with several apoptotic changes. These results are in harmony with (Al-Mzaien et al., 2015; Naqi, 2015) who established that lead produced neuropathological and biochemical alterations in the brain causing severe damage. All these changes were associated with positive caspase-3 reaction in most neurons with different degrees of astrogliosis. Our results showed that Pb-exposed animals exhibited brain edema which might be attributed to the disruption of blood brain barrier (BBB) function leading to disturbance in blood dynamics and escape of the fluid to the nervous tissue and these findings agree with Al-Mzaien et al. (2015). Extensive previous studies explained that the first step in the Pb neurotoxic effects might be primarily related to damage to the permeability of BBB through up regulation and activation of the transient receptor potential canonical channel TRPCI/TRPC4 channels in rat brain endothelial cells (Balbuena et al., 2012; Tobwala et al., 2014) suggested that BBB dysfunction is a contributing mechanism in lead neurotoxicity in a vitro model of the BBB. Yan et al. (2003) and O'Donnell et al. (2004) found that ischemia-related edema involves stimulation of brain Na-K-Cl co-transporter system facilitating edema formation and swelling of endothelial tissue cells. Thus, it is possible that those mechanisms contribute to the brain edema observed in this study. Since perivascular pericytes, astrocytes and adipocytes play a substantial role maintaining the function of the BBB (Xu and Ling, 1994; Guzik et al., 2007), perivascular swelling determined in Pb-exposed rats may represent swollen astrocytes, pericytes or adipocytes resulting in disruption of the BBB functions.

Abbott et al. (2006) reported that following lead exposure, astrocytes secrete variety of inflammatory cytokines into surrounding tissues, which further mediate the immune response including activation of microglia and macrophages and induce alternative adverse reactions which might eventually result in the destruction of BBB tight junctions. It has been hypothesized that inflammatory cytokines induce production of matrix metalloproteinases that degrade the extracellular matrix and basement membrane, in astrocytes, resulting in increased permeability of the BBB (Rosenberg, 2001). Astrocytes maintain the transendothelial electric resistance (TEER) of the BBB (Siddharthan et al., 2007). Kim et al. (2013) showed that lead toxicity in the BBB or brain microvascular endothelial cells might influence tight junction proteins. Balbuena et al. (2011) reported that lead reduces the expression of tight junction proteins and lowers TEER, causing changes in ion permeability at the BBB and brain interstitial fluid ion regulation. By penetrating the BBB, lead accumulates in astroglia cells, disrupting myelin sheath formation. Even in very little concentrations, lead affects neural excitation and memory-related neurotransmitter activity (Bressler et al., 1999;

Kim et al., 2015).

These vascular changes might impair nutrition and oxygen supply to both cerebral and cerebellar tissues. As neurons require relatively large quantities of O_2 due to their high metabolic rate (Gold et al., 2004). The degenerative changes observed in the neurons in addition to nuclear changes in the form of darkening and shrinking (pyknosis), abnormal chromatin distribution or nuclear fading (karyolysis) were seen in our study reflected a certain phase of apoptosis. These cells are considered metabolically inactive and in some instance dying cells. It might be due to ischemia resulting from substantial abnormalities in the capillary wall with subsequent disorders in the structural elements of the BBB (Donald et al., 2001). Biosynthesis and function of neuronal mitochondria activity is affected by lead with disruptive effects on synaptic transmission in the brain. Furthermore, lead affecting brain cells via excitotoxicity and apoptosis (Hel.Poblenz et al., 2000).

Most distorted cells appear with irregular outline and loss of the shape these changes can be correlated with the cytoskeletal disorganization observed by electron microscope. These cells manifested major ultrastructural changes in most organelles indicating cell degeneration. The increase of cytosolic calcium and alteration in mitochondrial permeability next to oxidative stress can cause mitochondrial injury which reflected on its function leading to rapid degeneration of the cells (Afifi and Embaby, 2016).

Mitochondrial alterations are observed as swollen vacuolated mitochondria with partial or complete loss of cristae which may be related to oxidative stress. The observed mitochondrial changes may be considered as early manifestation of apoptosis and an adaptive process to undesirable environments because of excess exposure of the cell to free radicals at the extent of intracellular organelles (Wakabayashi, 2002). It has been found that lead exposure interferes with astrocyte functions leading to the insufficient supply of energy from astrocytes to neurons as it causes morphological and functional changes in astrocytic mitochondria (Struzyñska et al., 2001). Mitochondrial dysfunction in astrocytes affects the survival of motor neurons (Cassina et al., 2008). Moreover, Lepper et al. (2010) stated that lead can bind to the sulfhydryl group of creatine kinase and pyruvate kinase and decrease their activity resulting in an insufficient supply of pyruvate and lactate from astrocytes to neurons. Lead can also act on cytochrome C and adenosine triphosphate synthase to cause dysfunction of the mitochondrial electron transport chain and generation of free radicals (Maiti et al., 2010). Accumulation of free radicals and ROS might impede the supply of energy to neurons eventually causing neuronal apoptosis (Lepper et al., 2010; Flora et al., 2012b; Mousa et al., 2015). It may be suggested that these observed alterations in the cellular integrity are due to excess Pb stored in the interneuronal spaces that inhibits oxygen utilization, thus reducing the production of the required level of ATP and modifying the morphology of the neuron to compensate for the available amount of energy present (Baranowska-Bosiacka and Hlynczak, 2003; Maiti et al., 2010). One of the pivotal role of astrocytes is to respond to injury via an intricate process known as reactive gliosis, which causes cellular damage or loss of normal neuroprotective functions in the CNS following injury, trauma, or disease (Aguzzi et al., 2013). Ultimately, the distorted shrunken cells seemed to be a result of damage structural and functional biosynthesis of cell proteins, nucleic acids, certain enzymes and various neurotransmitters (Carageorgiou et al., 2004).

Regarding the cytoplasmic vacuolation in the neurons of the Pb-treated rats and some of garlic-treated group (Gp III); it was a result of LPO theory, in addition to damage of the cell membrane as well as membranes of other damaged organelles from exposure to free radicals (Zarnescu et al., 2008). Such damage is specifically followed by an increase in the sodium permeability which surpasses the capacity of pump to extrude the sodium resulting in its accumulation within the cell followed by an increase in water content and swelling of the cell (Afifi and Embaby, 2016). The vacuolation in the surrounding neuropil might be attributed to the cells shrinkage and retraction of their processes secondary to cytoskeletal affection leaving pericellular spaces. They are indicative of neuronal death and are symmetrical with neuronal necrosis as seen in early stages of ischemic, hypoxic/ischemic, hypoglycemic and excitotoxic states (Auer and Sutherland, 2002). Scott et al. (2008) showed that the neuropil vacuoles represent the swollen neuronal processes and presynaptic nerve endings whereas the cytoplasmic vacuoles correspond with swollen mitochondria.

The axons changes were recorded as a component of a neuronal injury while the myelination's disruption was attributed to the changes in myelin basic protein secondary to membrane damage and axonal degeneration. Demyelination can occur as a response to axonal degeneration or secondary to the oxidative stress while dysmyelination was attributed to high water content in degenerating nerve causing intramyelinic edema and edematous splitting at various levels of the myelin lamella (Manzo et al., 1996). Watenaux et al. (2009) showed that the free radicals potentially deteriorate the oligodendrocytes and neurons causing damage to cell membrane and impairment of myelination.

Our study revealed several morphological changes in myelin of lead-exposed rat as well as degenerating myelin which signified by vacuoles in the myelin sheaths. These changes come in accordance with that of Dabrowska-Bouta et al. (2004) and Xu et al. (2009). Several mechanisms have been suggested such as diminished myelin associated lipids (Krigmann et al., 1972), myelin basic protein (Zawia and Harry, 1996) and myelin integral protein enzyme CNPase (Dabrowska-Bouta et al., 2004). The production and maintenance of myelin is essential to normal function of the CNS. Even small changes in myelin indices could lead to changes in conduction speed and signal timing which is critical for the proper function of integrated neuronal circuits (Felts et al., 1997). Altered fibers and overall myelin structure has been associated with a subsidence in cognitive function (Peters, 1996) and can influence motor function (Mattay et al., 2002). In addition, myelin abnormalities may lead to reduce propagation of nerve impulse (Hernández-Fonseca et al., 2009). Garlic-treated group (Gp III) still revealed ultrastructural alterations in myelin formation suggesting that the oligodendrocytes were not able to fully compensate the defect in myelination induced by lead.

Regarding the neuroglia, the enlarged processes of astrocytes may be attributed to lipid peroxidation theory and an increase in the sodium permeability resulting in its accumulation within the cell followed by increase in water content in the cell leading to its swelling (Panickar and Norenberg, 2005). The astrocytes were considered the primary cells involved in the regulation of the immune response to pathological processes in the brain (Liu et al., 2011). These cells played a critical role in neurotransmitter uptake and metabolism, neurotransmitter receptor expression, neurotrophic factor-secretion, secretion of extracellular matrix protein and maintenance of the extracellular balance of ions (Afifi and Embaby, 2016).

In the present study, the co-administration of spirulina with lead acetate resulted in a good degree of restoration of the altered levels of the investigated oxidative stress markers as detected by a significant reduction in MDA with the reversion of inhibited antioxidant enzymatic system (SOD and CAT), pronounced improvements in the ACHE activity and significantly reduced the elevated levels of caspase-3 observed in the lead-treated group (down regulation of caspase-3 gene expression). These results are in a harmony with those of Ponce-Canchihuamán et al. (2010); Gargouri et al. (2012); El-Tantawy (2016) and Khalil et al. (2018). Furthermore, examination of specimens obtained from animals treated with Pb concomitantly with spirulina showed remarkable improvement in the nerve cells and neuroglia and hardly ever the affected cells are noticed. These findings are in agreement with Gargouri et al. (2012) and Khalil et al., (2018). The protective effect of spirulina against Pb-induced oxidative stress could be attributed to its antioxidant contents, high degree of free radical scavenging activity and suppression of LPO. As spirulina contains many functional bioactive ingredients including phenolic phytochemicals (Jensen et al., 2015; Machu et al., 2015), phycobiliprotein C-phycocyanin (Finamore et al.,

2017), carotenoid, omega-3 and omega-6 polyunsaturated fatty acids, gamma-linolenic acid and complex of vitamins with antioxidant properties (Chopra and Bishnoi, 2008). The metallo-protective role of spirulina may be attributed due to the presence of β-carotene which has been suggested to be powerful single oxygen quenching, free radical scavenging and chain breaking during lipid LPO (Bangeppagari et al., 2014). For instance, selenium-containing phycocyanin from spirulina has strong free radical scavenger action against superoxide, hydrogen peroxide radical (Huang et al., 2007; Chu et al., 2010) which then enhance the macromolecular damage following the loss of neuronal function (Tobon-Velasco et al., 2013). Moreover, phycocyanins were found to act as neuroprotectants in rats treated with kainite, protecting the cerebellum against the oxidative stress-induced apoptosis (Hirata et al., 2000). Exogenous antioxidant such as β-carotene, ascorbic acid and α-tocopherol can be effective on neuronal cell protection due to the effect of ROS on neuronal cell damages and fast consumption of endogenous scavenging antioxidants (Varshosaz et al., 2014). Additionally, Santos et al. (2008) showed that ascorbic acid exerted neuroprotective action through decreasing LPO and increasing catalase activities. Furthermore, spirulina is recognized by its high digestible protein content (60–70% by dry weight) (Kulshreshtha et al., 2008). Indeed, spirulina is rich in many trace minerals (selenium, magnesium and manganese) which are essential cofactors for the different isoforms of the metalloenzymes. Therefore, it has a potential therapeutic agent for treating oxidative stress-induced diseases (Ghaeni and Roomiani, 2016).

Khalil et al. (2018) observed that spirulina supplementation could reduce lead levels in both blood and brain tissue in rats which was mostly related to the chelating capacity of spirulina for heavy metals (Elshazly et al., 2015; Bashandy et al., 2016). Indeed, spirulina has a rapid lead adsorption rate and high lead adsorption capacity and it enhances the elimination of heavy metals from the body (Banji et al., 2013). Spirulina ameliorated the effects of Pb on the brain tissue by facilitating the displacement of lead, resulting in reduced Pb accumulation in the body, through its potential antioxidant efficacy via its radical-scavenging ability (Banji et al., 2013). In addition to, ascorbic acid as a component of spirulina showed to curtail lead-induced oxidative stress and decreasing intestinal absorption as well as increasing renal lead clearance (Haridy et al., 2014). Besides, spirulina's restoration potency in the brain tissue was reliable even in terms of biochemical and histopathological outcomes. This implies that spirulina could serve as a biologically effective therapeutic agent that can enhance cell survival in the rat brains through caspase–3 down-expression and cell death suppression.

The biochemical data together with histopathological observations from Gp III have pronounced the efficiency of co-treatment with garlic to partially rescue brain from lead-induced damage. Garlic administration reversed the alterations induced by lead acetate in the MDA, antioxidant enzymes, ACHE activity, caspase-3 gene expression and these findings were similar to those in the previous studies (Yassin, 2005; Haridy et al., 2014; Manoj Kumar et al., 2016; Nasr et al., 2017; Saleh et al., 2018).

The protective role of garlic may be mediated through several actions; firstly by the prevention of LPO due to its thiol-containing compounds such as S-allyl cysteine (Massadeh et al., 2007), secondly, through prevention of excessive free radicals production due to its organo-sulfur, flavonoid aglycones and phenolic compounds contents, and these may be responsible for the antioxidant capabilities (Bozin et al., 2008), thirdly, through enhancing cellular antioxidant enzymes and activation of oxidant induced transcription factors due to its content of diallyl sulfide (Abdel-Daim and Abdou, 2015; Salem and Salem, 2016). Besides these properties, the other efficiency of garlic is perhaps due to the presence of compounds have free carboxyl (C═O) and amino (NH_2) groups in their structure (Taji et al., 2012). These biologically active compounds might chelate lead as they can easily permeate phospholipid membranes and reduce intracellular lead to enhance its excretion from the body resulting in reduced lead accumulation in soft tissue and blood (Haridy et al., 2014; Ebrahimzadeh-Bideskan et al., 2015). Previous studies revealed that administration of *A. sativum* has prophylactic efficacy in reducing the Pb burden in blood (Sadeghi et al., 2013; Saleh et al., 2018) and brain tissue (Manoj Kumar et al., 2016; Saleh et al., 2018) in lead-exposed animals. Furthermore, garlic extract enhanced the lead excretion in the urine and the feces of the exposed rats (Haridy et al., 2014). In addition to chelation, sulfur-containing amino acids such as S-allyl cysteine and S-allyl mercapto cysteine also prevent the gastrointestinal tract lead absorption, resulting in reduced blood lead level (Zhai et al., 2015; Haridy et al., 2014). Organo-sulfurs in garlic extract are known to neutralize H_2O_2 (Ide et al., 1997) and scavenge superoxide radicals (Kim et al., 2001), thereby preventing H_2O_2 induced cell damage. The prophylactic efficacy might be due to association of lipophilic organo-sulfur compounds of garlic with lead, resulting in its partial removal (Senapati et al., 2001). The antioxidant influence of garlic against lead induced toxicity in different tissues was reported (Manoj Kumar et al., 2016). In addition, our investigation showed that garlic co-administration reduced the elevated levels of caspase-3 induced by lead administration. Nasr et al. (2017) observed that garlic supplementation significantly down regulating the expression of proapoptotic marker proteins caspase-3 and Bax. These because garlic contained more than 200 chemical compounds including volatile oil with sulphur-containing allicin, allin, ajone, allinase, peroxidase and myrosinase (Hossain et al., 2014). By further investigation using immune-histochemistry, sections from Gp II revealed many apoptotic neurons with a strong positive reaction while spirulina co-treatment or garlic co-treatment showed their ameliorative effect.

5. Conclusion

Spirulina as well as garlic administration exhibited an ameliorating effect on the lead-induced neurotoxicity but spirulina had more effective protection than garlic. So, it is recommended that awareness should be focused on spirulina and antioxidants supplement; particularly in geographical areas where lead contamination is expected, as important protective measure for the neurotoxicity. Considering the mild degenerative changes still observed in some cells in this work, further intensive experimental and clinical study may be required to adjust the dose and time of treatment.

Conflict of interest

The authors declare no conflicts of interest.

References

Abbott, N.J., Rönnbäck, L., Hansson, E., 2006. Astrocyte-endothelial interactions at the blood-brain barrier. Nat. Rev. Neurosci. 7, 41–53.
Abdel-Daim, M.M., Abdou, R.H., 2015. Protective effects of diallyl sulfide and curcumin separately against thallium-induced toxicity in rats. Cell J. 17 (2), 379–388.
Abdulmajeed, W.I., Sulieman, H.B., Zubayr, M.O., Imam, A., Amin, A., Biliaminu, S.A., Oyewole, L.A., Owoyele, B.V., 2016. Honey prevents neurobehavioural deficit and oxidative stress induced by lead acetate exposure in male Wistar rats- a preliminary study. Metab. Brain Dis. 31 (1), 37–44. https://doi.org/10.1007/s11011-015-9733-6.
Abeer, M., 2012. Grape seed extract (Vitisvinifera) alleviate neurotoxicity and hepatotoxicity induced by lead acetate in male albino rats. J. Behav. Brain Sci. 2, 176–184.
Aebi, H., 1984. Catalase in vitro. Methods Enzymol. 105, 121–126.
Afifi, O.K., Embaby, A.S., 2016. Histological study on the protective role of ascorbic acid on cadmium induced cerebral cortical neurotoxicity in adult male albino rats. J. Microsc. Ultrastruct. 4, 36–45.
Aguzzi, A., Barres, B.A., Bennett, M.L., 2013. Microglia: scapegoat, saboteur, or something else? Science 339, 156–161.
Ahmed, M.B., Ahmed, M.I., Meki, A., Abd Raboh, N., 2013. Neurotoxic effect of lead on rats: relationship to Apoptosis. Int. J. Health Sci. Qassim Univ. 7 (2), 192–199.
Ahmed Refat, N.A.G., Abass, M.A., 2011. Efficacy of myrrh extract "Mirazid®" to reduce lead acetate toxicity in albino rats with special reference to cerebellum and testes. Life Sci. J. 8 (4), 406–414.
Al-Mzaien, A.K., Khalaf, O.H., AL- Neamah, G.A.K., Al-Naimi, R.A.S., 2015. Study some of the histopathological changes of acute, subacute and chronic lead acetate toxicity related to catalase activity in blood of adult male wistar rats. Kufa J. Vet. Med. Sci. 6

(2), 183–193.
Ani, M., Moshtaghie, A.A., Aghadavood, M., 2007. Protective effects of selenium and zinc on the brain acetylcholinesterase activity in lead intoxified rat. Res. Pharm. Sci. 2, 80–84.
Auer, R.N., Sutherland, G.R., 2002. Greenfield's Neuropathology, 7th edition. Arnold, London, pp. 233 Hypoxia and related conditions.
Balbuena, P., Li, W., Ehrich, M., 2011. Assessments of tight junction proteins occludin, claudin 5 and scaffold proteins ZO1 and ZO2 in endothelial cells of the rat blood-brain barrier: cellular responses to neurotoxicants malathion and lead acetate. Neurotoxicology 32, 58–67.
Balbuena, P., Li, W., Rzigalinshi, B.A., Ehrich, M., 2012. Malathion/oxon and lead acetate increase gene expression and protein levels of transient receptor potential chemical subunits TRPC1 and TRCP4 in rats endothelial cells of the blood – brain barrier. Int. J. Toxicol. 31 (3), 238–249.
Bancroft, J.D., Gamble, M., 2008. Theory and Practice of Histological Techniques, 6th ed. Churchill Livingstone/Elsevier, Philadelphia, PA.
Bangeppagari, M., Gooty, J.M., Tirado, J.O., Mariadoss, S., Thangaswamy, S., Maddela, N.R., Ortiz, D.R., 2014. Therapeutic efficiency of Spirulina against lead acetate toxicity on the fresh water fish Labeo rohita. Am. J. Life Sci. 2 (6), 389–394.
Banji, D., Banji, O.J., Pratusha, N.G., Annamalai, A.R., 2013. Investigation on the role of Spirulina platensis in ameliorating behavioural changes, thyroid dysfunction and oxidative stress in offspring of pregnant rats exposed to fluoride. Food Chem. 140, 321–331. https://doi.org/10.1016/j.foodchem.02.076.
Baranowska-Bosiacka, I., Hlynczak, A.J., 2003. The effect of lead ions on the energy metabolism of human erythrocytes in vitro. Comp. Biochem. Physiol. C Toxicol. Pharmacol. 134, 403–416.
Bashandy, S.A.E., El Awdan, S.A., Ebaid, H., Alhazza, I.M., 2016. Antioxidant potential of Spirulina platensis mitigates oxidative stress and reprotoxicity induced by sodium arsenite in male rats. Oxid. Med. Cell. Longev. 2016, 7174351. https://doi.org/10.1155/2016/7174351. 2016.
Borgesius, N.Z., de Waard, M.C., van der Pluijm, I., Omrani, A., Zondag, G.C., van der Horst, G.T., 2011. Accelerated age-related cognitive decline and neurodegeneration, caused by deficient DNA repair. J. Neurosci. 31, 12543–12553.
Bozin, B., Mimica-Dukic, N., Samojlik, I., Goran, A., Igic, R., 2008. Phenolics as antioxidants in garlic (Allium sativum L., Liliaceae). Food Chem. 111 (4), 925–929.
Bradford, M.M., 1976. A rapid and sensitive method for the quantitation of microgram quantities of protein utilizing the principle of protein-dye binding. Anal. Biochem. 72, 248–254.
Bressler, J., Kim, K.A., Chakraborti, T., Goldstein, G., 1999. Molecular mechanisms of lead neurotoxicity. Neurochem. Res. 24, 595–600.
Carageorgiou, H., Tzotzes, V., Pantos, C., Mourouzis, C., Zarros, A., Tsakiris, S., 2004. In vivo and in vitro effects of cadmium on adult rat brain total antioxidant status, acetylcholinesterase (Na^+, K^+)-ATPase and Mg^{2+}-ATPase activities: protection by L-cysteine. Basic Clin. Pharmacol. Toxicol. 94 (3), 112–118.
Cassina, P., Cassina, A., Pehar, M., Castellanos, R., Gandelman, M., de León, A., Robinson, K.M., Mason, R.P., Beckman, J.S., Barbeito, L., Radi, R., 2008. Mitochondrial dysfunction in SOD1G93A-bearing astrocytes promotes motor neuron degeneration: prevention by mitochondrial-targeted antioxidants. J. Neurosci. 28, 4115–4122.
Chaâbane, M., Ghorbel, I., Elwej, A., Mnif, H., Boudawara, T., Chaâbouni, S.E., Zeghal, N., Soudani, N., 2017. Penconazole alters redox status, cholinergic function, and membrane-bound ATPases in the cerebrum and cerebellum of adult rats. Hum. Exp. Toxicol. 36 (8), 1–13.
Chopra, K., Bishnoi, M., 2008. Antioxidant profile of spirulina: a blue-green microalga. In: Gershwin, M.E., Belay, A. (Eds.), Spirulina in Human Nutrition and Health. CRC Press, Boca Raton, pp. 101–118 2008.
Chu, W.L., Lim, Y.W., Radhakrishnan, A.K., Lim, P.E., 2010. Protective effect of aqueous extract from Spirulina platensis against cell death induced by free radicals. BMC Complement. Altern. Med. 2010 (10), 53.
Dabrowska-Bouta, B., Sulkowski, G., Struzyñska, L., Rafalowska, U., 2004. CNPase activity in myelin from adult rat brains after prolonged lead exposure in vivo. Chem. Biol. Interact. 150 (2), 171–178.
Deng, R., Chow, T.-J., 2010. Hypolipidemic, antioxidant, and anti-inflammatory activities of microalgae Spirulina. Cardiovasc. Ther. 28, 33–45. https://doi.org/10.1111/j.1755-5922.2010.00200.x.
Devi, C.B., Reddy, G.H., Prasanthi, R.P., Chetty, C.S., Reddy, G.R., 2005. Developmental lead exposure alters mitochondrial monoamine oxidase and synaptosomal catecholamine levels in rat brain. Int. J. Dev. Neurosci. 23 (4), 375–381.
Donald, M., Calton, W., Zachary, F., 2001. Special Veterinary Pathology, 3rd ed. Mosby, Inc., London, pp. 113.
Dribben, W.H., Creeley, C.E., Farber, N., 2011. Low-level lead exposure triggers neuronal apoptosis in the developing mouse brain. Neurotoxicol. Teratol. 33, 473–480.
Durak, D., Kalender, S., Uzun, F.G., Demir, F., Kalender, Y., 2010. Mercury chloride-induced oxidative stress and the protective effect of vitamins C and E in human erythrocytes in vitro. Afr. J. Biotechnol. 9 (4), 488–495.
Ebrahimzadeh-Bideskan, A., Sadeghi, A., Alipour, F., Kianmehr, M., 2015. The effects of ascorbic acid and garlic on bone mineralization in lead exposed pregnant rats. Zahedan J. Res. Med. Sci X(X): XX-XX.
El-Demerdash, F.M., Elagamy, E.I., 1999. Biological effects in Tilapia nilotica fish as indicators of pollution by cadmium and mercury. Int. J. Environ. Health Res. 9, 143–156.
El-Demerdash, F.M., Yousef, M.I., El-Naga, N.I., 2005. Biochemical study on the hypoglycemic effects of onion and garlic in alloxan-induced diabetic rats. Food Chem. Toxicol. 43 (1), 57–63.
Elshazly, M.O., Abd El-Rahman, S.S., Morgan, A.M., Ali, M.E., 2015. The remedial efficacy of Spirulina platensis versus chromium-induced nephrotoxicity in male sprague-dawley rats. PLoS One 1–16. https://doi.org/10.1371/journal.pone.0126780.
El-Tantawy, W.H., 2016. Antioxidant effects of Spirulina supplement against lead acetate-induced hepatic injury in rats. J. Tradit. Complement. Med. 6 (4), 327–331.
Ercal, N., Gurer-Orhan, H., Aykin-Burns, N., 2001. Toxic metals and oxidative stress part I: mechanisms involved in metal-induced oxidative damage. Curr. Top. Med. Chem. 1 (6), 529–539.
Felts, P.A., Baker, T.A., Smith, K.J., 1997. Conduction in segmentally demyelinated mammalian central axons. J. Neurosci. 17 (19), 7267–7277.
Finamore, A., Palmery, M., Bensehaila, S., Peluso, I., 2017. Antioxidant, immunomodulating, and microbial-modulating activities of the sustainable and eco-friendly Spirulina. Oxid. Med. Cell. Longev. 2017, 14. https://doi.org/10.1155/2017/3247528. Volume, Article ID 3247528.
Flora, S.J.S., Saxena, G., Mehta, A., 2007. Reversal of lead-induced neuronal apoptosis by chelation treatment in rats: role of reactive oxygen species and intracellular Ca^{2+}. J. Pharmacol. Exp. Ther. 322 (1), 108–116.
Flora, G., Gupta, D., Tiwari, A., 2012a. Toxicity of lead: a review with recent updates. Interdiscip. Toxicol. 5 (2), 47–58.
Flora, S.J., Gautam, P., Kushwaha, P., 2012b. Lead and ethanol co-exposure lead to blood oxidative stress and subsequent neuronal apoptosis in rats. Alcohol Alcohol 47, 92–101.
Gargouri, M., Ghorbel-Koubaa, F., Bonenfant-Magné, M., Magné, C., Dauvergne, X., Ksouri, R., Krichen, Y., Abdelly, C., El Feki, A., 2012. Spirulina or dandelion-enriched diet of mothers alleviates lead-induced damages in brain and cerebellum of newborn rats. Food Chem. Toxicol. 50, 2303–2310.
Ghaeni, M., Roomiani, L., 2016. Review for application and medicine effects of Spirulina, Spirulina platensis microalgae. J. Adv. Agric. Technol. 3 (2), 114–117.
Gill, K.D., Gupta, V., Sandhir, R., 2003. Ca^{2+}/calmodulin-mediated neurotransmitter release and neurobehavioural deficits following lead exposure. Cell Biochem. Funct. 21 (4), 345–353.
Gold, B.G., Voda, J., Yu, X., Gordon, H., 2004. The immunosuppressant FK506 elicits a neuronal heat shock response and protects against acrylamide neuropathy. Exp. Neurol. 187 (1), 160–170.
Gurer, H., Ercal, N., 2000. Can antioxidants be beneficial in the treatment of lead-poisoning? Free Radic. Biol. Med. 29, 927–945.
Guzik, T.J., Marvar, P.J., Czesnikiewicz-Guzik, M., Korbut, R., 2007. Perivascular adipose tissue as a messenger of the brain-vessel axis: role in vascular inflammation and dysfunction. J. Physiol. Pharmacol. 58 (4), 591–610.
Haridy, M., Al-Amgad, Z., Sakai, H., Mohi-Eldin, M., 2014. Ameliorating effects of garlic, calcium, and vitamin C on chronic lead toxicity in albino rats. Comp. Clin. Pathol. 23, 1215–1223. https://doi.org/10.1007/s00580-013-1765-x.
Hel.Poblenz, A.T., Medrano, C.I., Fox, D.A., 2000. Lead and calcium produce rod photoreceptor cell apoptosis by opining the mitochondrial permeability transition pore. J. Boil. Chem. 275, 12165–12184.
Hernández-Fonseca, J.P., Rincón, J., Pedreañez, A., Viera, N., Arcaya, J.L., Carrizo, E., Mosquera, J., 2009. Structural and ultrastructural analysis of cerebral cortex, cerebellum and hypothalamus from diabetic rats. Exp. Diabet. Res. 2009, 12. https://doi.org/10.1155/2009/329632. Art. ID 329632.
Hirata, T., Tanaka, M., Ooike, M., Tsunomura, T., Sakaguchi, M., 2000. La phycocyanine. J. Appl. Phycol. 12, 435–439.
Hossain, M.A., Akanda, M.R., Mostofa, M., Awal, M.A., 2014. Therapeutic competence of dried garlic powder (Allium sativum) on biochemical parameters in lead (Pb) exposed broiler chickens. J. Adv. Vet. Anim. Res. 1 (4), 189–195.
Hsu, S.M., Raine, L., Fanger, H., 1981. The use of antiavidin antibody and avidin-biotin peroxidase complex in immunoperoxidase techniques. Am. J. Clin. Pathol. 75, 816–821.
Huang, Z., Guo, B.J., Wong, R.N.S., Jiang, Y., 2007. Characterization and antioxidant activity of selenium-containing phycocyanin isolated from Spirulina platensis. Food Chem. 100, 1137–1143.
Ide, N., Nelson, A.B., Lau, B.H., 1997. Aged garlic extract and its constituents inhibit Cu2+ induced oxidative modification of low density lipoproteins. Plant Med. 63 (3), 263–264.
Jensen, G.S., Attridge, V.L., Beaman, J.L., Guthrie, J., Ehmann, A., Benson, K.F., 2015. Antioxidant and anti-inflammatory properties of an aqueous cyanophyta extract derived from arthrospira platensis: contribution to bioactivities by the non-phycocyanin aqueous fraction. J. Med. Food 18 (5), 535–541.
Khalaf, A.A., Moselhy, W.A., Abdel-Hamed, M.I., 2012. The protective effect of green tea extract on lead induced oxidative and DNA damage on rat brain. Neurotoxicology 33, 280–289.
Khalil, S.R., Khalifa, H.A., Abdel-Motal, S.M., Mohammed, H.H., Elewad, Y.H.A., Mahmoud, H.A., 2018. Spirulina platensis attenuates the associated neurobehavioral and inflammatory response impairments in rats exposed to lead acetate. Ecotoxicol. Environ. Saf. 157, 255–265.
Kim, K.M., Chun, S.B., Koo, M.S., Choi, W.J., Kim, T.W., Kwon, Y.G., Chung, H.T., Billiar, T.R., Kim, Y.M., 2001. Differential regulation of NO availability from macrophages and endothelial cells by the garlic component S-allylcysteine. Free Radic. Biol. Med. 30, 747–756.
Kim, J.H., Byun, H.M., Chung, E.C., Chung, H.Y., Bae, O.N., 2013. Loss of integrity: impairment of the blood-brain barrier in heavy metal-associated ischemic stroke. Toxicol. Res. 29, 157–164.
Kim, H.C., Jang, T.W., Chae, H.J., Choi, W.J., Ha, M.N., Ye, B.J., Kim, B.G., Jeon, M.J., Kim, S.Y., Hong, Y.S., 2015. Evaluation and management of lead exposure. Ann. Occup. Environ. Med. 27 (30), 1–9.
Kiran Kumara, B., Prabhakara Rao, Y., Noble, T., Kametris, W., McDowell, V.P., Sharada, R., Rajanna, B., 2009. Lead-induced alteration of apoptotic proteins in different regions of adult rat brain. Toxicol. Lett. 184, 56–60.
Knedel, M., Böttger, R., 1967. A kinetic method for determination of the activity of pseudocholinesterase (acylcholine acyl-hydrolase 3.1.1.8.). Klin. Wochenschr. 45 (6),

325–327.
Krigmann, M.R., Butt, S.A., Hogan, E.L., Shinkman, P.G., 1972. Morphological, neurochemical and behavioral correlates of lead intoxication and undernourishment in developing rats. Fed. Proc. 31 (Abstr. 2536), 665.
Kulshreshtha, A., Zacharia, A.J., Jarouliya, U., Bhadauriya, P., Prasad, G.B., Bisen, P.S., 2008. Spirulina in health care management. Curr. Pharm. Biotechnol. 9, 400–405.
Lamidi, I.Y., Akefe, I.O., 2017. Mitigative effects of antioxidants in lead toxicity. Res. Rep. Toxicol. 1 (1), 3.
Lepper, T.W., Oliveira, E., Koch, G.D., Berlese, D.B., Feksa, L.R., 2010. Lead inhibits in vitro creatine kinase and pyruvate kinase activity in brain cortex of rats. Toxicol. In Vitro 24, 1045–1051.
Liu, W., Tang, Y., Feng, J., 2011. Cross talk between activation of microglia and astrocytes in pathological conditions in the central nervous system. Life Sci. 89, 141–146.
Livak, K.J., Schmittgen, T.D., 2001. Analysis of relative gene expression data using real-time quantitative PCR and the 22DDCT. Methods 25, 402–408.
Lu, J., Ren, D.-F., Xue, Y.-L., Sawano, Y., Miyakawa, T., Tanokura, M., 2010. Isolation of an antihypertensive peptide from alcalase digest of Spirulina platensis. J. Agric. Food Chem. 58 (12), 7166–7171.
Mabrouk, A., Bel Hadj Salah, I., Chaieb, W., Ben Cheikh, H., 2016. Protective effect of thymoquinone against lead-induced hepatic toxicity in rats. Environ. Sci. Pollut. Res. Int. 23 (12), 12206–12215. https://doi.org/10.1007/s11356-016-6419-5.
Machu, L., Misurcova, L., Ambrozova, J.V., Orsavova, J., Mlcek, J., Sochor, J., Jurikova, T., 2015. Phenolic content and antioxidant capacity in algal food products. Molecules 20 (1), 1118–1133.
Maiti, A.K., Saha, N.C., Paul, G., 2010. Effect of lead on oxidative stress, Na^+K^+ATPase activity and mitochondrial electron transport chain activity of the brain of Clarias batrachus L. Bull. Environ. Contam. Toxicol. 84, 672–676.
Manoj Kumar, V., Henley, A.K., Nelson, C.J., Indumati, O., Prabhakara Rao, Y., Rajanna, S., Rajanna, B., 2016. Protective effect of Allium sativum (garlic) aqueous extract against lead-induced oxidative stress in the rat brain, liver, and kidney. Environ. Sci. Pollut. Res. 24 (2), 1544–1552. https://doi.org/10.1007/s11356-016-7923-3.
Manzo, L., Artigas, F., Martinez, R., Mutti, A., Bergamaschi, E., Nicotera, P., Tonini, M., Candura, S.M., Ray, D.E., Costa, L.G., 1996. Biochemical markers of neurotoxicity: a review of mechanistic studies and applications. Hum. Exp. Toxicol. 15 (Suppl. 1), S20–S35.
Massadeh, A.M., Al-Safi, S.A., Momani, I.F., Alomary, A.A., Jaradat, Q.M., AlKofahi, A.S., 2007. Garlic (Allium sativum L.) as a potential antidote for cadmium and lead intoxication: cadmium and lead distribution and analysis in different mice organs. Biol. Trace Elem. Res. 120, 227–234.
Mathew, B.C., Biju, R.S., 2008. Neuroprotective effects of garlic: areview. Libyan J. Med. 3, 16–20.
Mattay, V.S., Fera, F., Tessitore, A., Hariri, A.R., Das, S., Callicott, J.H., Weinberger, D.R., 2002. Neurophysiological correlates of age-related changes in human motor function. Neurology 58 (4), 630–635.
Morgan, A., Ibrahim, M.A., Galal, M.K., Ogaly, H.A., Abd-Elsalam, R.M., 2018. Innovative perception on using Tiron to modulate the hepatotoxicity induced by titanium dioxide nanoparticles in male rats. Biomed. Pharmacother. 103, 553–561.
Mousa, A.M., Al-Fadhli, A.S., Rao, M.S., Kilarkaje, N., 2015. Gestational lead exposure induces developmental abnormalities and up regulates apoptosis of fetal cerebellar cells in rats. Drug Chem. Toxicol. 38, 73–83.
Naqi, S.Z., 2015. A comparative study of the histological changes in cerebral cortex, hippocampus, cerebellum, pons & medulla of the albino rat due to lead toxicity. Int. J. Anat. Res. 3 (2), 1173–1178 ISSN 2321- 4287.
Nasr, N.E., Elmadawy, M.A., Almadaly, E.A., Abdo, W., Zamel, M.M., 2017. Garlic powder attenuates apoptosis associated with lead acetate-induced testicular damage in adult male rats. AJVS 54 (1), 70–78.
Nishikimi, M., Roa, N.A., Yogi, K., 1972. The occurrence of superoxide anion in the reaction of reduced phenazine methosulfate and molecular oxygen. Biochem. Biophys. Res. Commun. 46, 849–854.
O'Donnell, M.E., Tran, L., Lam, T.I., Liu, X.B., Anderson, S.E., 2004. Bumetanide inhibition of the blood-brain barrier Na-K-Cl cotransporter reduces edema formation in the rat middle cerebral artery occlusion model of stroke. J. Cereb. Blood Flow Metab. 24 (9), 1046–1056.
Ohkawa, H., Ohishi, N., Yagi, K., 1979. Assay for lipid peroxides in animal tissues by thiobarbituric acid reaction. Anal. Biochem. 95 (2), 351–358.
Onunkwor, B., Dosumu, O., Odukoya, O.O., Arowolo, T., Ademuyiwa, O., 2004. Biomarkers of lead exposure in petrol station attendants and auto-mechanics in Abeokuta, Nigeria: effect of 2-week ascorbic acid supplementation. Environ. Toxicol. Pharmacol. 17, 169–176.
Orrenius, S., Gogvadze, V., Zhivotovsky, B., 2007. Mitochondrial oxidative stress: implications for cell death. Annu. Rev. Pharmacol. Toxicol. 47, 143–183.
Panickar, K.S., Norenberg, M.D., 2005. Astrocytes in cerebral ischemic injury: morphological and general considerations. Glia 50 (4), 287–298.
Patra, R.C., Rautray, A.K., Swarup, D., 2011. Oxidative stress in lead and cadmium toxicity and its amelioration. Vet. Med. Int. 2011, 9 Article ID 457327.
Peters, A., 1996. Age-related changes in oligodendrocytes in monkey cerebral cortex. J. Comp. Neurol. 371 (1), 153–163.
Ponce-Canchihuamán, J.C., Pérez-Méndez, O., Hernández-Muñoz, R., Torres-Durán, P.V., Juárez-Oropeza, M.A., 2010. Protective effects of Spirulina maxima on hyperlipidemia and oxidative-stress induced by lead acetate in the liver and kidney. Lipids Health Dis. 9 (1), 35. https://doi.org/10.1186/1476-511X-9-35. 2010.
Pulido, M.D., Parrish, A.R., 2003. Metal-induced apoptosis: mechanisms. Mutat. Res. 533, 227–241.
Rashad, M.M., Galal, M.K., Abou-El-Sherbini, K.S., EL-Behairy, A.M., Gouda, E.M., Said, Z., Moussa, S.Z., 2018. Nano-sized selenium attenuates the developmental testicular toxicity induced by di-n-butyl phthalate in pre-pubertal male rats. Biomed. Pharmacother. 107, 1754–1762.
Richetti, S.K., Rosemberg, D.B., Ventura-Lima, J., Monserrat, J.M., Bogo, M.R., Bonan, C.D., 2011. Acetylcholinesterase activity and antioxidant capacity of zebrafish brain is altered by heavy metal exposure. Neurotoxicology 32 (1), 116–122.
Rosenberg, G.A., 2001. Matrix metalloproteinases in multiple sclerosis: is it time for a treatment trial? Ann. Neurol. 50, 431–433.
Sadeghi, A., Ebrahimzadeh-Bideskan, A.R., Alipour, F., Fazel, A.R., Haghir, H., 2013. The effect of ascorbic acid and garlic administration on lead induced neural damage in rat offspring's Hippocampus. Iran J. Basic Med. Sci. 16, 157–164.
Saleh, H.A., Abd El-Aziz, G.S., Mustafa, H.N., Saleh, A.H.A., Mal, A.O., Deifalla, A.H.S., Aburas, M., 2018. Protective effect of garlic extract against maternal and foetal cerebellar damage induced by lead administration during pregnancy in rats. Folia Morphol. 77 (1), 1–15.
Salem, N.A., Salem, E.A., 2016. Protective antioxidant efficiency of garlic against lead-induced renal and testicular toxicity in adult male rats. J. Heavy Met. Toxicity Dis. 1 (3:15), 1–7. https://doi.org/10.21767/2473-6457.100015.
Sansar, W., Bouyata, M., Ahboucha, S., Gamrani, H., 2011. Effects of chronic lead intoxication on rat serotoninergic system and anxiety behavior. Acta Histochem. 114 (1), 41–45.
Santos, L.F., Freitas, R.L., Xavier, S.M., Saldanha, G.B., Freitas, R.M., 2008. Neuroprotective actions of vitamin C related to decreased lipid peroxidation and increased catalase activity in adult rats after pilocarpine-induced seizures. Pharmacol. Biochem. Behav. 89 (1), 1–5.
Scott, C.A., Rossiter, J.P., Andrew, R.D., Jackson, A.C., 2008. Structural abnormalities in neurons are sufficient to explain the clinical disease and fatal outcome of experimental rabies in yellow fluorescent protein-expressing transgenic mice. J. Virol. 82 (1), 513–521.
Senapati, S.K., Dey, S., Dwivedi, S.K., Swarup, D., 2001. Effect of garlic (Allium sativum L.) extract on tissue lead level in rats. J. Ethnopharmacol. 76, 229–232.
Shalaby, M.A., Hammoda, A.A., 2015. Protective effect of Allium sativum juice and oil with vitamin E against testicular toxicity in rats. World J. Pharm. Pharm. Sci. 4 (1), 155–170.
Sharoud, M.N.M., 2015. Protective effect of Spirulina against paracetamol-induced hepatic injury in rats. J. Exp. Biol. Agric. Sci. 3 (1), 44–53.
Siddharthan, V., Kim, Y.V., Liu, S., Kim, K.S., 2007. Human astrocytes/ astrocyte-conditioned medium and shear stress enhance the barrier properties of human brain microvascular endothelial cells. Brain Res. 1147, 39–50.
Singh, P.K., Singh, M.K., Yadav, R.S., Nath, R., Mehrotra, A., Rawat, A., Dixit, R.K., 2017. Omega-3 fatty acid attenuates oxidative stress in cerebral cortex, cerebellum, and hippocampus tissue and improves neurobehavioral activity in chronic lead-induced neurotoxicity. Nutr. Neurosci. 1, 1–15. https://doi.org/10.1080/1028415X.2017.1354542.
Struzyñska, L., Bubko, I., Walski, M., Rafalowska, U., 2001. Astroglial reaction during the early phase of acute lead toxicity in the adult rat brain. Toxicology 165, 121–131.
Suszkiw, J.B., 2004. Presynaptic disruption of transmitter release by lead. Neurotoxicology 25, 599–604.
Taji, F., Shirzad, H., Ashrafi, K., Parvin, N., Kheiri, S., Namjoo, A., Asgari, A., Ansari, R., Rafieian-kopaei, M., 2012. A comparison between the antioxidant strength of the fresh and stale Allium sativum (garlic) extracts. Zahedan J. Res. Med Sci. 14 (5), 25–29.
Thuppil, V., Tannir, S., 2013. Treating lead toxicity: possibilities beyond synthetic chelation. J. Krishna Inst. Med. Sci. Univ. 2 (1), 4–31.
Tobon-Velasco, J.C., Palafox-Sanchez, V., Mendieta, L., Garcıa, E., Santamarıa, A., Chamorro-Cevallos, G., Limon, I.D., 2013. Antioxidant effect of Spirulina (Arthrospira) maxima in a neurotoxic model caused by 6-OHDA in the rat striatum. J. Neural Transm. 120, 1179–1189. https://doi.org/10.1007/s00702-013-0976-2.
Tobwala, S., Wang, H.J., Carey, J.W., Banks, W.A., Ercal, N., 2014. Effects of lead and cadmium on brain endothelial cell survival, monolayer permeability, and crucial oxidative stress markers in an in vitro model of the blood-brain barrier. Toxics 2 (2), 258–275. https://doi.org/10.3390/toxics2020258.
Varshosaz, J., Taymouri, S., Pardakhty, A., Asadi-Shekaari, M., Babaee, A., 2014. Niosomes of ascorbic acid and α-Tocopherol in the cerebral ischemia-reperfusion model in male rats. BioMed Res. Int. 2014, 9 ID 816103.
Wakabayashi, T., 2002. Mega mitochondria formation-physiology and pathology. J. Cell Mol. Med. 6, 497–538.
Wang, Y., Wang, S., Cui, W., He, J., Wang, Z., Yang, X., 2013. Olive leaf extract inhibits lead poisoning-induced brain injury. Neural Regen. Res. 8 (22), 2021–2029.
Watenaux, B., Rabinowitz, T., Needer, H., Auderix, O., 2009. Effects of cadmium exposure on the physiology of cerebellar neuron. Progress Neurophysiol. 48, 18–24.
Xu, J., Ling, E.A., 1994. Studies of the ultrastructure and permeability of the blood-brain barrier in the developing corpus callosum in postnatal rat brain using electron dense tracers. J. Anat. 184 (2), 227–237.
Xu, J., Ji, L.D., Xu, L.H., 2006. Lead-induced apoptosis in Pc 12 cells: involvement of p53, Bcl-2 family and caspase-3. Toxicol. Lett. 166, 160–167.
Xu, J., Yan, H.C., Yang, B., Tong, L.S., Zou, Y.X., Tian, Y., 2009. Effects of lead exposure on hippocampal metabotropic glutamate receptor subtype 3 and 7 in developmental rats. J. Negat. Results Biomed. 8 (1). https://doi.org/10.1186/1477-5751-8-5. Art. No. 5.
Yallapragada, P., Butler, J., Kumar, B., 2003. In vitro effect of lead on Na, K ATPase activity in different regions of adult rat brain. Drug Chem. Toxicol. 26, 117–124.
Yan, Y., Dempsey, R.J., Flemmer, A., Forbush, B., Sun, D., 2003. Inhibition of Na-K-Cl-cotransporter during focal cerebral ischemia decreases edema and neuronal damage. Brain Res. 961 (1), 22–31.
Yassin, M.M., 2005. Prophylactic efficacy of crushed garlic lobes, black seed or olive oils on cholinesterase activity in central nervous system parts and serum of lead intoxicated rabbits. Turk. J. Biol. 29, 173–180.

Zarnescu, O., Brehar, F.M., Chivu, M., Ciurea, A.V., 2008. Immunohistochemical localization of caspase-3, caspase-9 and Bax in U87 glioblastoma xenografts. J. Mol. Histol. 39, 561–569.
Zawia, N.H., Harry, G.J., 1996. Developmental exposure to lead interferes with glial and neuronal differential gene expression in the rat cerebellum. Toxicol. Appl. Pharmacol. 138 (1), 43–47.
Zhai, Q., Narbad, A., Chen, W., 2015. Dietary strategies for the treatment of cadmium and lead toxicity. Nutrients 7 (1), 552–571.
Zhang, J., Cai, T., Zhao, F., Yao, T., Chen, Y., Liu, X., Luo, W., Chen, J., 2012. The role of alpha-synuclein and tau hyperphosphorylation-mediated autophagy and apoptosis in lead-induced learning and memory injury. Int. J. Biol. Sci. 8, 935–944.